CATÓLICA

UNIVERSIDADE CATÓLICA PORTUGUESA | PORTO

Escola Superior de Biotecnologia

DAPTOMYCIN DELIVERY INTO THE EYE BY ENCAPSULATION INTO CHITOSAN COATED ALGINATE NANOPARTICLES

by

Joana Ribeiro Costa

November 2013

CATÓLICA

UNIVERSIDADE CATÓLICA PORTUGUESA | PORTO

Escola Superior de Biotecnologia

DAPTOMYCIN DELIVERY INTO THE EYE BY ENCAPSULATION INTO CHITOSAN COATED ALGINATE NANOPARTICLES

Thesis presented to *Escola Superior de Biotecnologia* of the *Universidade Católica Portuguesa* to fulfill the requirements of Master of Science degree in Biomedical Engineering

by

Joana Ribeiro Costa

Places: Escola Superior de Biotecnologia da Universidade Católica Portuguesa
Faculdade de Farmácia da Universidade do Porto
Instituto Superior de Ciências da Saúde - Norte

Supervision: Professor Manuela Pintado
Professor Bruno Sarmento

November 2013

Resumo

A endoftalmite bacteriana é uma inflamação ocular, resultante da introdução de um agente infeccioso no segmento posterior do olho. Grande parte das infeções são provocadas por bactérias Gram-positivas, tal como *Staphylococcus aureus* resistente à meticilina e *Staphylococcus epidermidis*. Atualmente, o tratamento de infeções oculares é dificultado pelas barreiras anatómicas e natureza delicada do interior do globo ocular. A aplicação de fármacos no próprio olho é uma solução não-invasiva, segura e menos dolorosa do que tratamentos cirúrgicos, a laser ou injeções oculares. A daptomicina é um novo péptido cíclico antimicrobiano, com atividade contra bactérias Gram-positivas, constituindo um poderoso agente no tratamento da endoftlamite bacteriana. Contudo, a aplicação tópica de daptomicina no olhoé limitada devido à rápida renovação do fluído ocular, requerendo formulações com propriedades mucoadesivas. Apesar da existência de nanopartículas de quitosano para encapsulamento de daptomicina, é necessária uma alternativa eficiente que possa melhorar as suas propriedades biológicas e farmacêuticas.

Neste trabalho, apresentam-se nanopartículas mucoadesivas de alginato revestidas com quitosano como possível sistema de libertação de daptomicina, uma vez que o alginato e o quitosano possuem diversas propriedades biológicas favoráveis ao prolongamento do tempo de residência pré-corneal do antibiótico, permitindo a acumulação e permeabilidade deste fármaco e integrando um método promissor para o tratamento tópico da endoftalmite bacteriana.

As nanopartículas foram preparadas através de pré-gelificação ionotrópica do alginato, seguido de complexação polielectrónica do quitosano e caracterizadas pelo seu tamanho, polidispersão e potencial zeta. As suas eficiências de encapsulação foram determinadas e a actividade antimicrobiana foi testada. Foi também avaliada, *in vitro*, a permeabilidade da daptomicina em células oculares.

As nanopartículas obtidas apresentam uma carga negativa, com tamanhos entre 382 e 421 nm e as eficiências de encapsulação apresentam valores entre 79 e 91%. A atividade antimicrobiana da daptomicina não sofreu alterações com o encapsulamento em nanopartículas. A permeabilidade ocular da daptomicina, *in vitro*, alcançou os 6% para células da córnea e 5% para células da retina, após 4 horas da aplicação.

Em conclusão, as nanopartículas obtidas são apropriadas para a libertação ocular de daptomicina, constituindo um potencial tratamento da endoftalmite bacteriana.

Abstract

Bacterial endophthalmitis is an ocular inflammation resultant from the introduction of an infectious agent into the posterior segment of the eye. Gram-positive bacteria such as methicillin-resistant *Staphylococcus aureus* and *Staphylococcus epidermidis* are the main cause of majority of endophthalmitis cases. Currently, treatment of bacterial infections and inflammation in the eye poses the dilemma of anatomic barriers and the delicate nature of the interior of the eye. Local drug applied to the eye represents a non-invasive, safe and less painful solution than surgery, laser treatments or eye injections. Daptomycin is a novel acidic cyclic lipopeptide antimicrobial agent with activity against Gram-positive organisms, including methicillin-resistant *Staphylococcus aureus*, becoming a powerful agent for treatment of bacterial endophthalmitis, though, topical administration of daptomycin directly into the eye is limited due to the rapid ocular fluid turn-over, requiring formulations with mucoadhesive properties. In spite of the existence of chitosan nanoparticles as daptomycin carrier, it is required an efficient alternative that may improve their biological and pharmaceutical properties. In the present project, mucoadhesive chitosan-coated alginate nanoparticles are proposed as effective delivery systems for daptomycin through ocular epithelium, taking advantage of the favourable biological properties of alginate and chitosan to prolong precorneal residence time of the antibiotic, enhancing drug accumulation and permeation.

Nanoparticles were prepared by ionotropic pre-gelation of an alginate core followed by chitosan polyelectrolyte complexation, characterized regarding particle size, polydispersity and zeta potential, encapsulation efficiency was determined, and antimicrobial activity was also tested after encapsulation of the antibiotic. Also, i*n vitro* ocular permeability of daptomycin-loaded nanoparticles was tested using cell culture models.

Formulated daptomycin-loaded chitosan coated alginate nanoparticles were negatively charged and sized between 380-420 nm, suitable for ocular application. Encapsulation efficiencies were between 79 and 92%. Antibacterial activity of daptomycin against major microorganisms responsible for bacterial endophthalmitis was not affected by encapsulation into nanoparticles. In vitro permeability was up to 6% for corneal cells and 5% for retinal cells after 4 hours.

In conclusion, obtained nanoparticles are suitable for daptomycin delivery in the eye and seem to be a promising vehicle for bacterial endophthalmitis treatment.

Acknowledgments

Firstly, I would like to acknowledge my supervisors, Professor Manuela Pintado and Professor Bruno Sarmento, for all the help and guidance given throughout the course of this work, providing all the conditions to carry out this work.

I wish to express my sincere gratitude to Nádia Silva, thank you for all your precious assistance, patience and wise advises that helped me to overcome many obstacles during this work.

Also, I would like to offer my regards to my lab colleagues: to Eduardo Costa and Sara Silva, thank you for all the help in the laboratory; to Francisca Araújo, thank you for the assistance with the cell growing work; to Adriana Pereira and Inês Montenegro, thank you for gentleness and for receiving me so well.

To my dear classmates, Marta Godinho, Paulo Dias and Pedro Sousa, thank you for all the shared ideas and moments of joy through this master degree.

Moreover, I would like to thank to all my friends for the all their friendship, care and support given every day. Special thanks to Ana Serra, Daniela Rodrigues, Fernando Moreira, Liliana Barbosa, Lúcia Rios, Luís Adães and Sebastião Almeida for your interest and encouragement throughout this work.

Finally, this project would not have been possible without my family support, particularly my parents, who have always supported and understood me, a special thanks for all your love and care.

Contents

List of Figures

List of Tables

List of Abbreviations

5-FU - 5-Fluorouracil

DMEM – Dulbecco's Modified Eagle Medium

EMA - European Medicines Agency

FDA - Food and Drug Administration

HBSS – Hanks Balanced Salt Solution

HCE – Human Corneal Epithelial

MIC – Minimum Inhibitory Concentration

MRSA – Methicillin-resistant *Staphylococcus aureus*

MRSE – Methicillin-resistant *Staphylococcus epidermidis*

MSSA – Methicillin-susceptible *Staphylococcus aureus*

Pen - Penicillin

PRSP – Penicillin-resistant *Streptococcus pneumonia*

RPE – Retinal Pigment Epithelium

RP-HPLC - Reverse-Phase High Performance Liquid Chromatography

TER – Transepithelial resistance

VA - Vancomycin

VRE – Vancomycin-resistant enterococci

VRSA – Vancomycin-resistant *Staphylococcus aureus*

I. Introduction

1. Anatomy of the eyeball

The human eye is a small organ that provides sense of sight, allowing the perception of shapes, colors and dimensions around the world. In spite of constant environmental changes, the eye has the ability to adapt to new conditions. It also works as an external barrier of the body, continuously threatened by foreign bodies that can lead to eye diseases, so it is also a very sensitive structure.

A wide diversity of eye diseases affects millions of people around the world and has devastating effects on individuals, leading to visual injury and possible ocular blindness that instigate a decline in quality of life (Short, 2008).

The eyeball occupies the anterior part of the orbit and its rounded shape is disrupted anteriorly, where it bulges outward, representing about one-sixth of the total area of the eyeball (Drake *et al*., 2010).

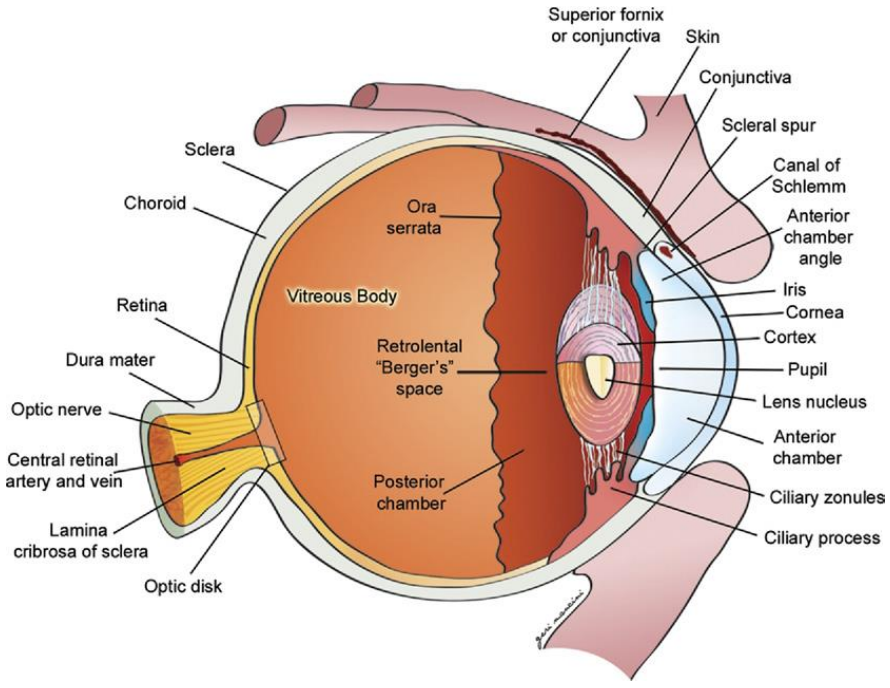

Figure 1.1 – Representation of the gross anatomy of the globe (Malhotra *et al*., 2011).

Surrounding the internal components of the eyeball are the walls of the eyeball. They consist of three layers: the outer fibrous layer, the middle vascular layer and the inner neural layer (Drake *et al*., 2010), as represented in Figure 1.1. Other important structures include the lens, which separates the vitreous body from the aqueous humor, and the conjunctiva (Presland, 2007; Silva, 2012).

1.1. Fibrous layer

The fibrous layer of the eyeball has two components – the sclera, that covers the posterior and lateral parts the eyeball and the cornea, which covers the anterior part (Drake *et al*., 2010).

The sclera extends from the limbus at the margin of the cornea anteriorly to the optic nerve posteriorly, where it is contiguous with the dural sheath of the optic nerve (Malhotra *et al*., 2011). It acts as a protective layer, maintains intraocular pressure and serves as the attachment site for extraocular muscles (Malhotra *et al*., 2011).

Continuous with the sclera, anteriorly is the transparent cornea (Drake *et al*., 2010). The cornea is a transparent avascular connective tissue that acts as the primary infectious and structural barrier of the eye (DelMonte and Kim, 2011). The human cornea consists of five layers: corneal epithelium, basement membrane, Bowman's layer, stroma, Descemet's membrane and endothelium (Hornof *et al*., 2005). The corneal epithelium is composed of two to three cell layers of flattened superficial cells, two to three cell layers of wing cells, and a single layer of columnar basal cells (Hornof *et al*., 2005). The superficial cells adhere to one another via desmosomes and the cells are encircled by tight junctions (Klyce and Crosson, 1985). Due to these tight junctions, the corneal epithelium represents the ratelimiting barrier for the permeation of hydrophilic drugs, whereas the stroma and endothelium offer very little resistance to transcorneal permeation (Hornof *et al*., 2005).

The composition of the sclera and the cornea is identical; however, one layer is clear and the other is opaque (Presland, 2007). This is because of the structural organization of the collagen fibers: in the cornea, collagen fibers are arranged in highly regular *laminae*; in the sclera, the fibers appear interwoven and extend in all directions (Presland, 2007).

1.2. Vascular layer

Inside the fibrous layer is the vascular/ muscular layer (Presland, 2007). The vascular layer of the eyeball consists of three continuous parts – the choroid, the ciliary body and the iris (Drake *et al*., 2010). Anteriorly the choroid becomes continuous with ciliary body, which, in turn, is continuous with the iris (Presland, 2007).

The choroid is a thin, highly vascular, pigmented layer consisting of smaller vessels adjacent to the retina and larger vessels more peripherally (Drake et al., 2010). The inner surface of the choroid is smooth and firmly attached to the retinal pigment epithelium (RPE) and the outer surface is roughened and attached to the sclera in the region of the optic nerve (Malhotra *et al*., 2011). It supplies oxygen and nutrients to outer layers of the retina and the structures of the anterior chamber (Presland, 2007).

The ciliary body extends from the posterior insertion of the iris to merge with the choroid at the *ora serrate*, a junction between the retina and the ciliary body, and forms a complete ring around the eyeball (Malhotra *et al*., 2011). It is made up of ciliary muscle and ciliary processes. The ciliary muscle consists of smooth muscle fibers arranged longitudinally, circularly and radially, which controls the size and shape of the lens due to contraction (Drake *et al*., 2010; Presland, 2007). The ciliary processes are longitudinal ridges projecting from the inner surface of the ciliary body and produce aqueous humour (Drake *et al*., 2010; Presland, 2007).

The iris is a thin, contractile, pigmented diaphragm that divides the anterior ocular compartment into anterior and posterior chamber with a central aperture, the pupil (Malhotra *et al*., 2011), as represented in Figure 1.2. Controlling the size of the pupil are smooth muscle fibers within the iris:

- the sphincter pupillae muscle, innervated by parasympathetics, which contraction of its fibers decreases the pupillary opening;

- the dilator pupillae muscle, innervated by the sympathetics, which contraction of its fibers increases the pupillary opening (Drake *et al*., 2010).

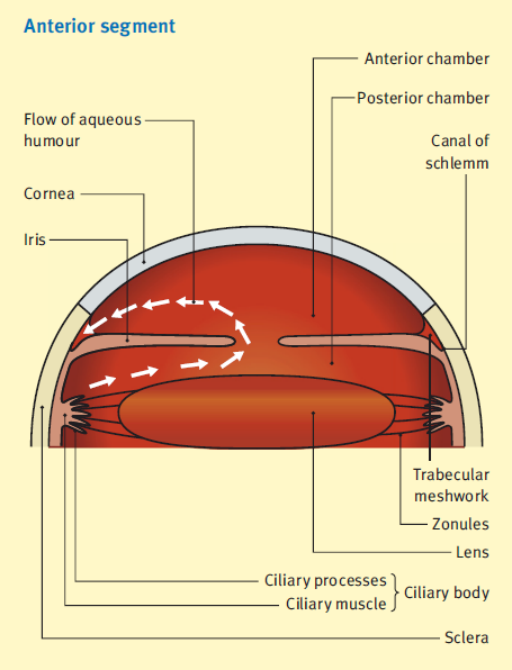

Figure 1.2 – Anterior segment of the human eyeball (Presland 2007)

1.3. Neural Layer

The innermost layer of the eyeball is the neural layer, or retina (Presland, 2007). It consists of two layers: posteriorly and laterally is the optic part of the retina, which is sensitive to light; anteriorly is the nonvisual part, which covers the internal surface of the ciliary body and the iris. The junction between these parts is the *ora serrate*, an irregular line (Drake *et al*., 2010). The optic part of the retina consists of two layers:

- the pigmented layer, firmly attached to the choroid and continues anteriorly over the internal surface of the ciliary body and iris;

- the neural layer, which can be further subdivided into its various neural components, is only attached to the pigmented layer around the optic nerve and at the *ora serrata* (Drake *et al*., 2010).

Among the functions of RPE cells, is the transport of nutrients from the vascular choroid, the formation of the blood-retinal barrier and the absorption of scattered light (Dunn *et al*., 1995). RPE cells are also thought to release factors that have trophic effects upon the neural retina, promoting both the differentiation and survival of photoreceptors (Sheedlo *et al*., 1992).

1.4. Lens

The lens is a transparent biconvex elastic disc, attached circumferentially to muscles associated with the outer wall of the eyeball, that allows the lens to change its refractive ability to maintain visual acuity and separates the aqueous from the vitreous (Drake *et al*., 2010; Malhotra *et al*., 2011).

1.5. Vitreous body and aqueous humour

The vitreous body is a gelatinous substance that provides the eye structural support (Presland, 2007). It occupies the space between the lens and the retina and is mainly composed by water, collagen fibrils, soluble proteins, salts and hyaluronic acid (Malhotra *et al*., 2011).

The aqueous humour is a water based substance secreted by the ciliary processes into the posterior chamber (Presland, 2007).

1.6. Conjunctiva

The conjunctiva is a thin transparent membrane that covers the full extent of the posterior surface of each eyelid before reflecting onto the outer surface of the eyeball, and attaches to the eyeball at the junction between the sclera and the cornea (Ludwig, 2005; Drake *et al*., 2010). It is a multilayered, non-keratinezed epithelium containing the goblet cells, which segregate the mucus, a layer that hydrates, cleanses, lubricates and serves as defense against pathogens (Robinson and Mlynek, 1995; Le Bourlais *et al*., 1998). Conjunctiva is involved in the formation and maintenance of the precorneal tear film, and in protection of the eye (Järvinen *et al*., 1995).

2. Bacterial endophthalmitis

Bacterial endophthalmitis is an ocular inflammation, resulting from the introduction of an infectious agent into the posterior segment of the eye (Callegan et al., 2002). It remains one of the most upsetting diagnoses in ophthalmology as it causes permanent harm to delicate photoreceptor cells of the retina and frequently leads to partial or total blindness within a few

days of inoculation, in spite of proper therapeutic intervention (Callegan *et al*., 2002; Kernt and Kampik, 2010). The major symptoms are redness, photophobia, pain and visual loss. The outcome of the infection differs from patients and depends on many factors as the age, immune status, condition of the eye upon presentation, virulence of the infecting organism, antibiotic susceptibility or the time between infection and therapy (Callegan *et al*., 2007). However it frequently runs a potentially devastating course, leaving very limited visual function so the early diagnosis and treatment with antimicrobial agents are important to optimize visual outcome (Kernt and Kampik, 2010). Progression of the disease may lead to panophthalmitis (inflammation of the entire eye), corneal infiltration and perforation, and affection of orbital structures (Kernt and Kampik, 2010).

2.1. Types of endophthalmitis

According to the origin of the infection, endophthalmitis is classified into two types: exogenous and endogenous endophthalmitis.

2.1.1. Exogenous endophthalmitis

Exogenous endophthalmitis is the most common form of the condition and the infectious source associated is external to the body (Peyman *et al*., 2004). According to the route of infection, exogenous endophthalmitis can be classified as post-operative endophthalmitis and post-traumatic endophthalmitis.

Post-operative endophthalmitis is a consequence of intraocular surgery and has been reported as a consequence following nearly every type of ocular surgery, but is most common following cataract surgery that is by far the most frequently performed procedure (Callegan *et al*., 2007; Kernt and Kampik 2010). Onset may be acute, in first week after surgery, or chronic, after one month (The College of Optometrists, 2011). The etiologic agents of acute post-operative endophthalmitis are generally microorganisms of the eyelid margin and preocular tear film that includes *Staphylococcus aureus*, *Staphylococcus epidermis*, *Streptococcus* species, *Bacillus* species, *Pseudomonas* species and *Aspergillus* species (Peyman *et al*., 2004; Kunimoto *et al*., 1999). However, post-operative endophthalmitis is not always infective as it can be caused by retention of foreign material (as cotton fibers) or toxic substances (The College of Optometrists, 2011).

Post-traumatic endophthalmitis represent about 25% of all endophthalmitis cases and are the result of open globe injuries (Kernt and Kampik, 2010). The microbiologic spectrum of post-traumatic endophthalmitis includes *Staphylococcus epidermis*, *Propionibacterium acnes*, *Bacillus cereus* and *Pseudomonas* and *Streptococcus* species (Kernt and Kampik, 2010).

2.1.2. Endogenous endophthalmitis

Endogenous endophthalmitis occurs when the interior of the eye is seeded with bacteria from a distant site of infection, most often affecting immunocompromised individuals, those with prolonged indwelling medical devices and intravenous drug abusers (Callegan *et al*., 2007). It accounts for approximately 5% to 10% of endophthalmitis cases (Kernt and Kampik, 2010). Common causes of endogenous bacterial endophthalmitis include *Staphylococcus aureus*, *Bacillus cereus*, *Escherichia coli*, *Neisseria meningitides*, *Klebsiella* species and the opportunistic fungus *Candida albicans* (Callegan *et al*., 2002).

2.2. Treatment

Treatment of endophthalmitis, either exogenous or endogenous, remains a challenge as in one hand the prognosis of endophthalmitis is often poor and on the other hand the treatment of bacterial infections and inflammations in the interior of the eye is still a dilemma (Callegan *et al*., 2007; Kernt and Kampik, 2010).

When endophthalmitis is initially suspected and the pathogen organism is not typically known, the choice of antimicrobial agent must be made empirically, taking the risk that posterior culture results do not correlate adequately to the previous selection of antibiotics (Callegan *et al*., 2002). The recommend management includes the direct injection of antibiotics into the vitreous, because the blood-ocular barrier may prevent their adequate penetration into the vitreous at levels above the minimal inhibitory concentration for the infecting pathogen when these drugs are administered systemically (Callegan *et al.*, 2007).

Common antibiotics used in the treatment of endophthamitis include vancomycin, aminoglycosides, cephalosporins and fluoroquinolones (Callegan *et al*., 2007). Benz and co-workers (Benz *et al*., 2004) studied the susceptibilities of organisms involved in the bacterial endophthalmitis infection to the antimicrobial agents and concluded that the most active

antibiotics for Gram-positive organisms were: vancomycin 100%, ciprofloxacin 68.3%, ceftazidime 63.6% and cefazolin 66.8%. For Gram-negative organisms, sensitivities were the following: ciprofloxacin 94.2%, amikacin 80.9%, ceftazidime 80.0%, and gentamicin 75.0%. With this data it is reasonable to conclude that no single antibiotic provides coverage for all of the microrganisms isolated from eyes with endophthalmitis, therefor the most commonly procedure is the intravitreal injections with combined antibiotics as vancomycin and amikacin or ceftazidime (Benz *et al*., 2004; Callegan et al. 2007).

3. Resistance to antibiotics

Challenging the treatment of infections due to Gram-positive pathogens is the development and prevalence of resistance to currently available antibiotics (Jeu and Fung, 2004). Data from the European Antimicrobial Resistance Surveillance System demonstrate the increase in prevalence of methicillin-resistant *Staphylococcus aureus* (MRSA) bacteraemias in most countries, which are associated with increased mortality, morbidity and costs compared with methicillin-susceptible strains (Enoch *et al*., 2007). The infection by glycopeptide resistant Enterococcus is also an increasing problem, particularly with strains of *Enterococcus faecium.* In 2011, resistance of *E. faecium* isolates to vancomycin exceeded 20% in Portugal and 34% in Ireland (European Centre for Disease Prevention and Control, 2013). In United States of America, national surveys of intensive care units indicate that VRE (Vancomycin Resistant Enterococci) represented less than 1% of enterococcal isolates in 1990 but currently exceed 30% (Mckinnell *et al*., 2012).

The current epidemic infections has led to the increased use of vancomycin in patients and an increase in vancomycin Minimum Inhibitory Concentrations (MICs) has been observed, encouraging the Clinical and Laboratory Standards Institute to lower the upper limit of vancomycin susceptibility from 4 µg/ mL to 2 µg/ mL in 2006 (Watkins et al., 2012).

Agents with activity against Gram-positive organisms for treatment of nosocomial infections attributed to vancomycin-resistant strains recently introduced include linezolid, quinupristin-dalfopristin and tigecycline but have revealed new resistance problems as well (Enoch et al., 2007; Jeu and Fung, 2004). The changes in the susceptibility profile of Gram-positive pathogens have escalated the need for more innovative drugs, such as daptomycin (Jeu and Fung, 2004).

4. Daptomycin

Daptomycin, the first of a new class of antibiotics, is a novel acidic cyclic lipopeptide antimicrobial agent with activity against Gram-positive organisms (Jeu and Fung, 2004; Enoch *et al*., 2007). It is a fermentation product of *Streptomyces roseosporus* that was discovered in the early 1980s and was approved by the Food and Drug Administration (FDA) in 2003 and by the European Medicines Agency (EMA) in 2006 for the treatment of complicated skin and soft tissue infections caused by gram-positive organisms at 4 mg/kg once daily (Enoch *et al*., 2007).

Daptomycin is characterized by a cyclic 13-amino acid anionic nucleus and an amide-linked lipophilic 10-amino acid fatty acyl side chain, as represented in Figure 1.3 (Jeu and Fung, 2004).

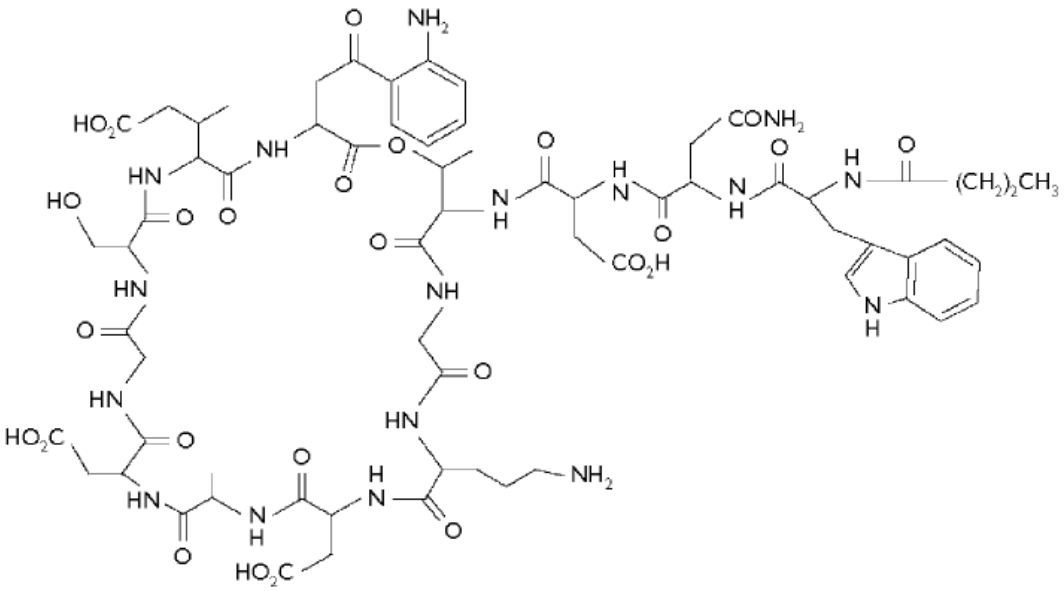

Figure 1.3 – Chemical Structure of Daptomycin (Jeu and Fung, 2004).

4.1. Mechanism of action and pharmacology

The proposed mechanism for daptomycin action involves calcium-dependent binding of the lipophilic tail of daptomycin to the bacterial cell membrane (Enoch *et al*., 2007). After binding to phospholipid vesicles in the planar bilayer membrane, daptomycin inserts the acyl fatty acid chain into the bacterial cytoplasmic membrane, triggering oligomerization of membrane proteins to form ion channels, transmembrane pores and other aggregate structures across the plasma membrane (Jeu and Fung, 2004). The binding of calcium ions in the core decapeptide

lactone promotes further insertion of the daptomycin tail into the phospholipid layer, and induces conformational changes that increase the amphiphaticity and reduce the charge, allowing daptomycin to interact with neutral or acidic membranes (Jeu and Fung, 2004). Formation of transmembrane structures disrupts the membrane functional integrity, resulting in an efflux of intracellular potassium ions, membrane depolarization, and cell death (Jeu and Fung, 2004; Enoch *et al*., 2007). It has also been demonstrated that daptomycin strongly inhibits the synthesis of lipoteichoic acid that is found in Gram-positive organisms (Enoch *et al*., 2007).

Daptomycin does not cross the blood-brain barrier or penetrate the cerebrospinal fluid, its metabolism is minimal and its excretion in predominantly renal (Enoch *et al*., 2007).

4.2. Spectrum of activity and susceptibility

Daptomycin has activity against a broad range of Gram-positive aerobic and anaerobic bacteria, but no activity against Gram-negative bacteria (Enoch *et al*., 2007). Its major advantage is the bactericidal activity against species that are resistant to other antibiotics, including MRSA, penicillin-resistant *Streptococcus pneumoniae* (PRSP), vancomycin-resistant enterococci (VRE) and vancomycin-resistant *Staphylococcus aureus* (VRSA) (Nguyen et al., 2006). *In vitro* susceptibility data, i.e. minimal inhibitory concentrations, are presented in Table 1.1.

The European Committee on Antimicrobial Susceptibility Testing established the breakpoints for both staphylococci and streptococci strains (excluding *S. pneumonia*): ≤1 mg/L is susceptible and > 1 mg/ L is resistant. In the USA has been defined a breakpoint of 4 mg/L for enterococci (Enoch *et al.*, 2007).

As a natural lipopetide antibiotic active against Gram-positive bacteria, particularly methicillin-resistant strains, daptomycin can be an interesting antibacterial tool to combat ocular infections caused by these microorganisms (Silva, 2012).

Table 1.1 – MIC_{50} and MIC_{90} of daptomycin among different species isolated. Adapted from Enoch *et al*. (2007).

Organism	MIC_{50} (mg/L)	MIC_{90} (mg/L)
Staphylococcus aureus	0.125	0.5
MSSA[(a)]	0.25	0.5
MRSA	0.25	0.5
Staphylococcus epidermidis	0.25	0.5
MRSE	0.25	0.5
Enterococcus faecalis	1	2
E. faecalis (VA[(b)] resistant)	1	2
Enterococcus faecium	2	8
E. faecium (VA[(b)] resistant)	1	2
Streptococcus pyogenes	0.0125	0.06
Streptococcus peneumoniae	0.25	0.5
S. pneumoniae (pen[(c)]resistant)	0.125	0.25

[(a)] MSSA: abbreviation for methicillin susceptible *Staphylococcus aureus*;
[(b)] VA: abbreviation for vancomycin; [(c)] Pen: abbreviation for penincillin;

5. Routes of drug delivery to the eye

There are different possible routes of drug delivery into the ocular tissues, and the selection of the route of administration depends primarily on the target tissue (Urtti, 2006). The various routes of ocular drug delivery are represented in Figure 1.4.

Physicochemical properties of drugs, namely lipophilicity, solubility, molecular size, shape, charge and degree of ionization may affect the route and rate of permeation in cornea (Le Bourlais *et al*., 1998).

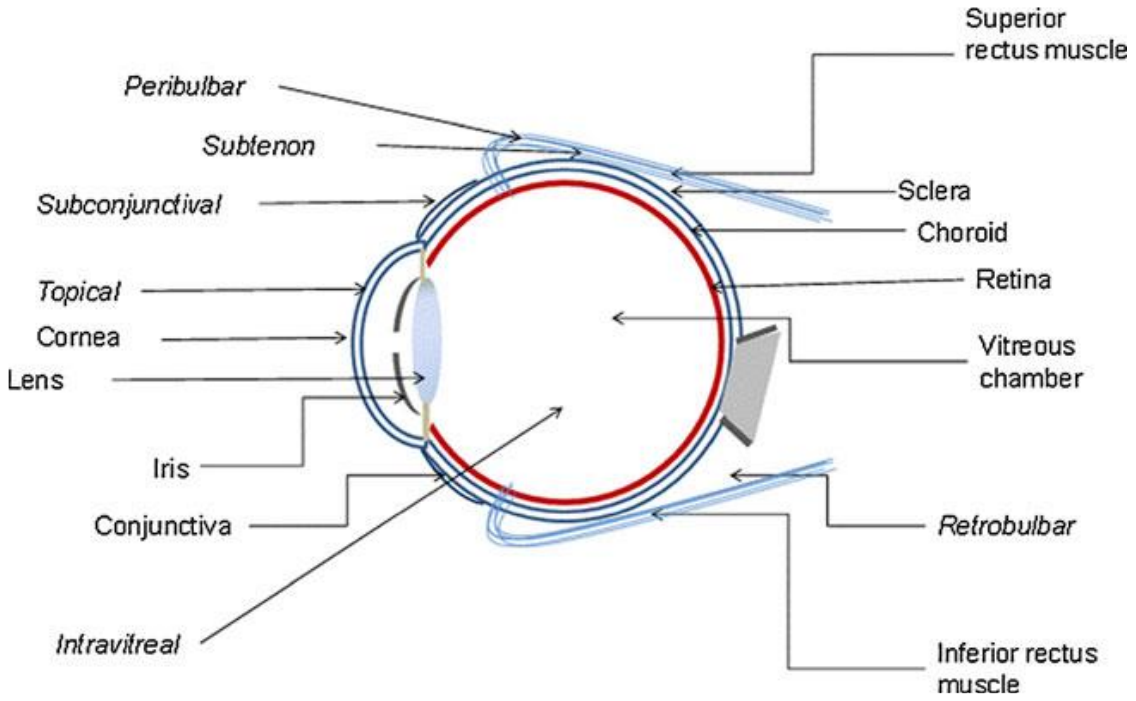

Figure 1.4 – Different routes of ocular drug delivery and their anatomical location (Gaudana *et al*., 2010).

5.1. Topical delivery

Topical administration, mostly in form of eye drops, is employed to treat anterior segment diseases and the site of action is usually different layers of the cornea, conjunctiva, sclera and the other tissues of the anterior segment such as the iris and ciliary body (Gaudana *et al*., 2010). However, the topical route is inefficient in delivering therapeutic concentrations of a drug to the posterior segment of the eye, owing to rapid drainage through the nasolacrimal ducts, low permeability of the corneal epithelium, systemic absorption and the blood-aqueous barrier (Thrimawithana *et al*., 2011). Typically, less than 5% of the applied drug penetrates the cornea and reaches intraocular tissues (Le Bourlais *et al*., 1998).

5.2. Systemic delivery

Following systemic administration, the blood aqueous barrier and the blood-retinal barrier are the major barriers for anterior and posterior segments ocular drug delivery, respectively, and restrict the entry of the therapeutic agents from blood (Gaudana *et al*., 2010). However, owing to the toxicity and delivery concerns, intravenous administration is not very common in treating ocular disorders (Gaudana *et al*., 2010).

5.3. Intravitreal delivery

Intravitreal injection of drugs into the eye involves direct injection of the formulation, in the form of solution, particles, suspension, depot or implants, into the posterior segment through the pars plana, a flat area in the ciliary body (Thrimawithana *et al*., 2011). Direct drug administration into the vitreous offers distinct advantage of more straightforward access to the vitreous and retina, providing increased drug concentrations at the neural retina and minimizing systemic side effects (Urtti, 2006; Thrimawithana *et al*., 2011). However, with intravitreal injections the drug distribution in the vitreous is non-uniform, as small molecules can rapidly distribute through the vitreous, whereas the diffusion of larger molecules is restricted, depending on the pathophysiological condition and the molecular weight of the administered drug (Gaudana *et al*., 2010).

5.4. Periocular delivery

The periocular route includes subconjunctival, subtenon, retrobulbar and peribulbar administration and is comparatively less invasive than intravitreal route, being considered the least painful and the most efficient route of drug delivery to the posterior eye (Gaudana *et al*., 2010; Thrimawithana *et al*., 2011). Drug solutions are placed in close proximity to the sclera which results in high retinal and vitreal concentrations as the periocular route enables the deposition of molecules against the external surface of the sclera because it is made up of fibrous tissue, which offers less resistance to permeability of drugs (Gaudana et al., 2010; Thrimawithana *et al*., 2011).

6. Ocular barriers

The delivery of drugs to the posterior segment of ocular tissue is prevented by ocular anatomical and physiological constraints, which include the relative impermeability of the corneal epithelial membrane, tear dynamics, nasolacrimal drainage and the high efficiency of the blood-ocular barrier (Ding, 1998).

6.1. Drug loss from the ocular surface

The exposed part of the eye is covered by a thin fluid layer, the so-called precorneal tear film that consists of a superficial lipid layer, a central aqueous layer and an inner mucus layer (Ludwig, 2005). After administration of eye drops, the most common dosage form, the flow of lacrimal fluid removes instilled compounds from the surface of the eye and the excess volume is flown to the nasolacrimal duct rapidly in a couple of minutes (Urtti, 2006).

In addition, most of small molecular weight drugs are absorbed into systemic circulation after few minutes, decreasing the drug concentration in lacrimal fluid extensively (Urtti, 2006). In this case, attempts to overcome the toxicity associated with the high initial concentration without a requirement for frequent dosing form is a challenging task, particularly in case of potent drugs (Ding, 1998).

6.2. Nasolacrimal drainage system

Corneal epithelium limits the drug absorption from the lacrimal fluid into the eye and is the major factor for drug loss that leads to poor ocular bioavailability. It is also the major route of entry into the circulatory system for drugs that are applied through topical administration (Urtti, 2006; Ding, 1998). The most apical corneal epithelial cells form tight junctions that limit the drug permeation, therefore lipophilic drugs have higher permeability in the cornea than the hydrophilic drugs (Urtti, 2006).

Furthermore, the systemic exposure through nasolacrimal drainage after topical administration can be sufficiently high to cause systemic toxicity (Ding, 1998).

6.3. Blood-ocular barrier

The eye is protected from xenobiotics in the blood stream by blood-ocular barriers and, consequently, the delivery of drugs to the retina from the peripheral circulation is also limited by this membrane impermeability (Urtti, 2006; Park *et al*., 2012). These barriers consist of two parts: blood-aqueous barrier and the blood-retina barrier, which are formed by complex tight junctions of retinal blood vessels and the RPE (Urtti, 2006; Park *et al*., 2012).

It is known that the anterior blood-eye barrier prevents the access of albumin into the aqueous humor and limits the access of hydrophilic drugs from plasma into the aqueous humor,

but these blood-eye barriers have not been extensively characterized in terms of drug transporter and metabolic enzyme expression (Urtti, 2006). The blood-ocular barrier can be overcome by intravitral injections of drugs, however this route of administration is associated with several problems, including risks of endophthalmithis (Bochot *et al*., 2000).

Cell culture models of ocular barriers constitute potent systems to explore the architecture, barrier function and regulation of ocular barriers *in vitro*. Monolayers of ARPE-19 cells have become a well-established *in vitro* model of the outer blood-retinal barrier (Hornof *et al*, 2005). This cell line was characterized by Dunn and colleagues (Dunn *et al*., 1996), who concluded that it has structural and functional properties characteristic of RPE cells *in vivo* and suggest that this cell line is valuable for in vitro studies of RPE physiology.

7. Ophthalmic drug delivery systems

Ocular drug delivery remains among the most challenging approaches to the administration of therapeutic agents to human body, being circumvent of the ocular protective barriers in order to achieve therapeutically effective concentration of drugs in the intraocular tissues the ultimate task (Liu *et al*., 2012).

An idyllic ocular drug delivery system should hold the following characteristics:

- provide controlled and sustained release profile to keep therapeutic concentration of the medicine for a lengthy period of time, in order to shrink the regularity of administration;

- be precise on targeting and sustained holding in the sickly tissues, with the aim of increase therapeutic efficiency and moderate side effects;

- be patient friendly delivery routes that reduce or eradicate side effects resulting directly from these administration methods (Liu *et al*., 2012).

The ultimate goals are to improve relevant drug-related parameters, such as pharmacokinetics, pharmacodynamics, non-specific toxicity, immunogenicity, biorecognition and to improve therapeutic efficacy (Diebold and Calonge, 2010).

Controlled drug delivery systems aim to deliver drugs at predetermined rates and predefined periods of time, targeting drugs to a desirable group of cells. In this perspective, micro- and nano-scale intelligent systems can maximiza the efficacy of therapeutic treatments (Safari and Zarnegar, 2012)

Nanocarriers, such as nanoparticles, have the capacity to deliver ocular drugs to specific target sites, holding the promise to revolutionize the therapy of many eye diseases (Diebold and Calonge, 2010).

7.1. Nanoparticles for ocular drug delivery

Nanoparticles are particles of less than 1μm diameter, prepared from natural or synthetic materials, such as polymers (Hans and Lowman, 2002).

Nanoparticles can be prepared in different sizes, charge and other physicochemical features, conferring great versatility upon them; also, as a biomedical application, they should be biologically compatible with living tissues by not producing toxic, injurious or immunologic responses in them (Diebold and Calonge, 2010).

Nevertheless, the same properties that make nanoparticles attractive for biomedical applications may become reactive in biological systems and develop toxicity: for instance, smaller size nanoparticles are preferred for better interactions at the cellular level. However, smaller nanoparticles have larger surface area per unit mass, which may mean higher reactivity and consequently, cell or tissue toxicity (Diebold and Calonge, 2010).

Nanoparticles have the great advantage of higher drug loading capacity and higher stability in biological fluids and during storage compared to other similar carriers (Eljarrat-Binstock *et al*., 2007).

Considering the fact that the cornea and conjunctiva have a negative charge, it was proposed that the use of mucoadhesive polymers, which may interact intimately with these extraocular structures, and increase the concentration and residence time of the associated drug (Motwani *et al*., 2008).

Among the wide variety of natural polymers reported in literature, alginate and chitosan seem to have most of the desirable characteristics for the formulation of drug loaded nanoparticles for ocular delivery (Motwani *et al*., 2008).

7.1.1. Alginate

Alginate is a random, linear and anionic polysaccharide consisting of linear copolymers of α-L-guluronate and β-D-mannuronate residues (Motwani *et al*., 2008). Commercial alginate is primarily extracted from marine algae such as *Laminaria hyperborean*, *Ascophyllum nodosum* and *Macrocystis pyrifera* and its molecular variability depends on the source of algae, tissue from which alginate is extracted and also the season of crop harvesting (Liew *et al*., 2005). The composition, sequence of polymer blocks and molecular weight of alginate is also important, as these factors determine the physical properties of the gel formed (Liew *et al*., 2005).

Alginate is widely used in the pharmaceutical, cosmetic and food industry and their significance in the biomedical area is increasing, including the development of drug delivery systems and a variety of oral and topical pharmaceutical formulations, as they are biodegradable, non-toxic, biocompatible and mucoadhesive (Motwani *et al*., 2008). It has also been used in a variety of oral and topical pharmaceutical formulations and it has been specifically used for aqueous microencapsulation of drugs (Motwani et al., 2008). Alginate polymers are also hemocompatible, have not been found to accumulate in any major organs and show evidence of *in vivo* degradation (Motwani et al., 2008).

The use of alginate in the encapsulation of drugs for sustained release is already wide-ranging. For instance, Sangeetha and colleagues (Sangeetha *et al*., 2007) formulated sodium alginate nanospheres of amphotericin B by controlled gellification method and yielded particles with 419.6 nm approximately that were found to have better antifungal activity when compared to the free drug and yielded sustained release; Zahoor and colleagues (Zahoor *et al*., 2007) studied the chemotherapeutic potential of alginate nanoparticle-encapsulated econazole and other antitubercular drugs against murine tuberculosis and concluded that alginate nanoparticles are the ideal carriers of these drugs, and also reduce dosing frequencies.

Alginate has also been used in several ocular delivery systems, either alone or in combination with other materials (Zhu *et al*., 2012). Liu and co-workers (Liu *et al.*, 2008) formulated an ophthalmic delivery system for gatifloxacin using alginate as gelling agent in combination with hydroxypropyl methylcellulose as a viscosity-enhancing agent and concluded that the mixture can be used as an *in-situ* gelling vehicle to enhance ocular bioavailability; the same authors (Liu *et al*., 2012) developed a composite collagen hydrogel containing protein encapsulated alginate microspheres for ocular applications that supported corneal epithelial cell growth, adequate

mechanical strength, and excellent optical clarity for possible use as therapeutic lens for drug delivery or use as corneal substitute for transplantation.

An extensive literature review allows to conclude that, despite the many ocular applications of alginate already developed, none of them includes the use of alginate as a base for formulation of a potential topical delivery systems of antibiotics to the eye.

7.1.2. Chitosan

Chitosan is a cationic polysaccharide and a deacetylated form of chitin, which is the second-most abundant polymer in nature after cellulose (de la Fuente *et al*., 2010; Alonso and Sánchez, 2003). Many applications have been found in the food, pharmaceutical, textile, agriculture, water treatment and cosmetics industries (Kong *et al*., 2010).

Chitosan exhibits several favorable biological properties, such as biodegradability, non-toxicity, biocompatibility and mucoadhesiveness (de Campos et al., 2004). Furthermore, antimicrobial activity of chitosan has also been demonstrated against many bacteria, filamentous fungi and yeast (Kong *et al*., 2010).

Chitosan base is soluble in acidic solutions wherein it becomes protonated; this positive charge of the chitosan molecule enables its interaction with polyanions, a process that has been used to obtain complexes as well as micro and nanoparticulate drug delivery systems (Alonso and Sánchez, 2003).

Because of all these favorable properties and also the ability to increase mucosal epithelia permeability, chitosan is a very promising biomaterial in ophthalmology (Alonso and Sánchez, 2003). Moreover, it shows pseudoplastic and viscoelastic properties, desirable for ocular drug administration (de la Fuente *et al*., 2010).

Chitosan-alginate polyionic complexes are formed through the ionic gelation via interactions between the carboxyl groups of alginate and the amine groups of chitosan (Motwani *et al*., 2008). This complex revealed to protect the encapsulant and limit the release of encapsulated materials more effectively than either alginate or chitosan alone (Motwani *et al*., 2008).

7.1.3. Alginate-Chitosan polyelectrolyte complexes

Nanoparticles made of opposite surface charged polymers have potential application in ophthalmic delivery. Low stability and encapsulation efficiency have been observed with capsules formed by an alginate polymer (anionic), but these problems can be overcome using cationic polymers such as chitosan (Nagarwal *et al*., 2012). In fact, the combination of chitosan and sodium alginate has been widely investigated and is considered to be the most interesting chitosan-polyanion complex for colloidal carrier systems (Patil *et al*., 2011; Motwani *et al*., 2007). The formed nanoparticles are biocompatible, biodegradable, non-toxic, and capable to sustain the release of encapsulated materials more efficiently than either alginate or chitosan alone, which represents the major advantage for using chitosan coated alginate nanoparticles (Motwani *et al*., 2007; Nagarwal *et al*., 2012).

Motwani and colleagues (Motwani *et al*., 2007) designed chitosan-sodium alginate nanoparticles as a new vehicle for the prolonged topical ophthalmic delivery of gatifloxacin that revealed a fast release during the first hour followed by a more gradual release during a 24-hour period; Nagarwal and co-workers (Nagarwal *et al*., 2012) developed chitosan coated sodium alginate-chitosan nanoparticles loaded with 5-Fluorouracil for ophthalmic delivery and *in-vivo* study in rabbit eye showed a great level of 5-FU in aqueous humor and high bioavailability resulting from the mucoadhesiveness.

Despite the evident advantages of using alginate in combination with chitosan for ocular applications, it is possible to conclude, after a general literature review, that alginate-chitosan polymeric nanoparticles have never been used for encapsulation of antimicrobial peptides, such as daptomycin.

Topical administration of daptomycin into the eye by encapsulation into chitosan nanoparticles has been studied by Silva (Silva *et al*., 2013), concluding that chitosan nanoparticles are suitable for delivering daptomycin into the eye. However, considering the capacity of alginate-chitosan polymeric nanoparticles to sustain the release of encapsulated material more efficiently than chitosan nanoparticles, the development of chitosan coated sodium alginate nanoparticles for encapsulation of daptomycin and subsequent topical administration into the eye constitutes a promising system for treatment of bacterial endophthalmitis

8. Objectives

The general objective of the present study is the improvement of an efficient topical delivery system of the novel antibiotic daptomycin to the posterior segment of the eye for the treatment of bacterial endophthalmitis. In order to achieve this objective, daptomycin will be encapsulated into chitosan coated alginate nanoparticles and its potential as ocular drug delivery system will be evaluated.

The specific objectives of this study include:

- Preparation of feasible alginate-chitosan nanoparticles for encapsulation of daptomycin;
- Physicochemical characterization of obtained nanoparticles and determination of drug loading capacity;
- Determination of Minimal Inhibitory Concentrations (MICs) against some Gram-positive pathogens responsible for bacterial endophthalmitis for daptomycin solution and encapsulated daptomycin in alginate-chitosan nanoparticles, and establish the comparison between both;
- Determination of the permeability of daptomycin solution and daptomycin-loaded nanoparticles in ARPE-19 and HCE cells monolayers;

II. Material and Methods

1. Materials

Daptomycin (94.9% of purity) was offered by Cubist Pharmaceuticals, Inc. (Massachusetts, USA) and Novartis Pharma AG (Basel, Switzerland). Alginic acid sodium salt from brown algae (sodium alginate), low molecular chitosan (deacetylation degree of 85%) and acetic acid at 99.7% were acquired from Sigma-Aldrich® (Missouri, USA). Calcium chloride dehydrate ($CaCl_2 \cdot 2H_2O$) was obtained from Merck (Darmstadt, Germany). Ultra-pure water was achieved in our lab with a Millipore™ (Massachusetts, USA) water purification system.

Acetonitrile, trifluoroacetic acid and triethylamine were also purchased from Sigma-Aldrich® (Missouri, USA). Nanoparticles were characterized with ZetaPALS equipment from Brookhaven Instruments Corporation (New York, USA) and drug loading capacity was determined using a Beckman Coulter System Gold HPLC system (California, USA).

Nutrient Broth and Nutrient Agar mediums were obtained from Lab M™ (Lancashire, United Kingdom) and Mueller-Hinton medium was acquired from Biokar Diagnostics (Beauvais, France). 96-well microplates were purchased from Nunc (Roskilde, Denmark).

For cell culture assays, Dulbecco's Modified Eagle Medium (DMEM) was purchased from PAA Laboratories (Pasching, Austria), Hanks Balanced Salt Solution (HBSS) was obtained from Biowhittaker (Verviers, Belgium), tissue culture test plates were acquired from Orange Scientific (Braine-l' Alleud, Belgium) and 6-well- format cell culture transwell inserts were purchased from BD Falcon (New Jersey, USA).

2. Development of chitosan coated sodium-alginate nanoparticles

2.1. Unloaded nanoparticles

The main purpose for previous formulation of unloaded nanoparticles is to achieve the best conditions of alginate-chitosan nanoparticles formulation to be used in daptomycin-loaded nanoparticles.

Unloaded chitosan coated alginate nanoparticles were prepared following the method of Zahoor *et al.* (2005) with slight modifications, using cation-induced controlled gellification of alginate. Nanoparticles were prepared from dilute alginate solution by inducing an ionotropic pre-gelation with calcium counter ions, followed by polyelectrolyte complex coating with chitosan.

For that purpose, 0.5 mL of $CaCl_2$ and 2 mL of chitosan solutions were added dropwise to 9.5 mL of alginate solution, followed by stirring for 30 minutes. The pH of the final solution was adjusted to 3.5-3.6, in order to keep the conditions of formulation of unloaded and loaded nanoparticles similar, as at these pH values daptomycin is positively charged and alginate is negatively charged, allowing the polyelectrolyte interaction between them. Nanoparticles were stored at room temperature overnight.

Based on the concentrations of alginate, chitosan and $CaCl_2$ used by Zahoor (Zahoor *et al*., 2005), it were first prepared the stock solutions. Alginate stock solutions were prepared by dissolving different amounts of alginate into ultrapure water, achieving concentration of 0.3, 0.6, 0.9 and 1.2 mg/mL. Chitosan was dissolved overnight in different acetic acid solutions (also prepared with ultrapure water), achieving stock solutions with concentrations of 0.2, 0.5 and 1.0 mg/ mL. At last, stock solutions of $CaCl_2$ were set with ultrapure water, with concentrations of 1.14 and 2.64 mg/ mL.

Table 2.1 - Different concentrations of alginate, chitosan and $CaCl_2$ used in the final solution to prepare unloaded chitosan coated sodium alginate nanoparticles.

Alginate Concentration (mg/mL)	Chitosan Concentration (mg/mL)	$CaCl_2$ Concentration (mg/mL)	Alginate: Chitosan mass ratio
0.24	0.08	0.11	1: 0.07
0.48	0.04	0.11	1: 0.018
	0.08	0.06	1: 0.035
		0.11	1: 0.035
	0.17	0.11	1: 0.07
0.71	0.08	0.11	1 : 0.024
0.95	0.08	0.11	1 : 0.018

After nanoparticle formation, alginate achieved final concentrations of 0.24, 0.48, 0.71 and 0.95 mg/ mL, chitosan achieved the concentrations of 0.04, 0.08 and 0.17 mg/mL and $CaCl_2$

solutions the final concentrations of 0.06 and 0.11 mg/ mL, as suggested by Zahoor (Zahoor et al., 2005). In all cases, it was guaranteed that chitosan and $CaCl_2$ concentrations were not superior to alginate concentration. The different combinations of final concentrations used to prepare the nanoparticles are presented in table 2.1.

Considering the physicochemical characteristics of the nanoparticles obtained using these formulations, it was then prepared another set of unloaded nanoparticles using stock solutions of alginate with 0.1 mg/ mL, stock solutions of chitosan with 0.1, 0.3 and 0.5 mg/ mL and stock solutions of calcium chloride of 1.0, 1.5 and 2.0 mg/ mL. From these stock solutions, new nanoparticles were obtained with the concentrations in the final solution presented on table 2.2.

All alginate nanoparticles were characterized for their size, polidispersity index and zeta potencial.

Table 2.2 - Different concentrations of alginate, chitosan and $CaCl_2$ used in the final solution to prepare unloaded chitosan coated alginate nanoparticles, after preliminary study.

Alginate Concentration (mg/mL)	Chitosan Concentration (mg/mL)	$CaCl_2$ Concentration (mg/mL)	Alginate: Chitosan mass ratio
0.08	0.02	0.04	1 : 0.05
		0.06	
		0.08	
	0.05	0.04	1 : 0.14
		0.06	
		0.08	
	0.08	0.04	1 : 0.22
		0.06	
		0.08	

2.2. Daptomycin-loaded nanoparticles

To prepare daptomycin-loaded nanoparticles, 0.5 mL of $CaCl_2$ (0.04 mg/mL in the final solution) was added to 9.5 mL of alginate (0.08 mg/mL in the final solution) containing different amounts of daptomycin, as described in table 2.3. The pH was adjusted to 3.5 - 3.6, because at this pH value, daptomycin molecules have an electric positive charge and the

alginate solution has a negative charge, enhancing electrical binding between alginate and daptomycin (Silva *et al*., 2013; Tønnesen and Karlsen, 2002).

After that, 2.0 mL of chitosan solution (0.02 mg/mL in the final solution) were then added, followed by stirring for 30 minutes and nanoparticles were stored at room temperature overnight. Alginate, chitosan and calcium chloride concentrations were chosen based in the optimal particle size, polydispersity index and zeta potential results obtained for unloaded nanoparticles.

Table 2.3 - Different concentrations of alginate, chitosan and $CaCl_2$ and daptomycin mass in the final solution used to prepare chitosan coated nanoparticles loaded with daptomycin.

Alginate (mg/ mL)	Chitosan (mg/ mL)	$CaCl_2$ (mg/mL)	Daptomycin (mg/ mL)	Alginate : Daptomycin mass ratio
0.08*	0.02 *	0.04 *	10 *	1 : 0.01
			20 *	1: 0.03
			40 *	1: 0.05
			80 *	1 : 0.1
			160 *	1 : 0.2
			330 *	1 : 0.4

* Concentration in the final nanoparticle suspension

An aliquot of nanoparticle suspension was transferred into a cuvette for size, polydispersity index and zeta potential characterizing in the ZetaPALS equipment. Posterior, daptomycin loaded nanoparticles were recovered by centrifugation 5000 rpm for 120 minutes and the supernatants were collected for determination of daptomycin loading capacity through the reverse-phase high performance liquid chromatography (RP-HPLC).

3. Physicochemical characterization of nanoparticles

Both loaded and unloaded alginate nanoparticles were submitted to deep physico-chemical characterization. Particle size, polydispersity index and Zeta potential were determined using a ZetaPALS equipment (Brookhaven Instruments Corporation, New York, USA).

Particle size and polydispersity index were determined by dynamic light scattering, using a 90º scattering angle and a temperature of 25ºC for the analysis. Zeta potential was measured by phase analysis light scattering technique with Smoluchowski model, using the same cell. Samples were submitted to 6 runs with 20 cycles each, at the temperature of 25ºC.

4. Determination of encapsulation efficiency of daptomycin in nanoparticles

The amount of daptomycin entrapped in alginate nanoparticles was calculated by estimating the amount of free drug in the supernatant after centrifugation of nanoparticles (Zahoor *et al.*, 2005)

The daptomycin encapsulation efficiency was calculated as the percentage of drug entrapped in alginate nanoparticles compared with the initial amount of drug, using the following equation (1):

$$(1)\ \text{Encapsulation Efficiency (\%)} = \frac{\text{Final concentration of drug - drug concentration in supernatant}}{\text{Final concentration of drug}} \times 100$$

The daptomycin concentration in supernatant was determined by RP-HPLC, using the method of Martens-Lobenhoffer *et al*. (2008) with slightly modifications.

4.1. Instrumentation

The HPLC system consisted of a Beckman Coulter System Gold comprising a System Gold 508 Autosampler, a System Gold 126 Solvent Module, a System Gold 168 detector and a Gecko 2000 Column Oven. The analytical column used was a Zorbax Eclipse XDB-C8 150mm x 4.6mm 5 µm particle size (Agilent Technologies, Böblingen, Germany).

4.2. Chromatography method setup

The mobile phase for the chromatographic separation of daptomycin was mixed from pure acetonitrile and buffer solution, which consisted of 20mM trifluoroacetic acid and 15mM triethylamine, resulting in a pH of about 3.5 (Martens-Lobenhoffer *et al*., 2008). Both solutions were filtered under vacuum and sonicated for 15 minutes.

The applied gradient starts as 30% acetonitrile, rises to 40% in 5 minutes, then set constant until 11 minutes. After 11 minutes the column is flushed for 3 minutes with 100% acetonitrile. The flow rate was constant to 0.700 mL/min and the column temperature was adjusted to 30ºC. The volume injected was 50 µL. Detention took place at a wavelength of 224 nm (Martens-Lobenhoffer *et al*., 2008).

4.3. Preparation of calibration solutions and calibration function

First, it was prepared a daptomycin stock solution in ultra-pure water, achieving the final concentration of 5000 µg/mL. From the dilution of this stock solution, a working solution of 500 µg/mL was obtained and this one was also diluted, acquiring another 50 µg/mL working solution.

From the stock solution with final concentration of 500 µg/mL, the calibration solutions with concentrations of 500, 400, 350, 250, 140, 70 and 35 µg/mL were prepared. From the working solution with the final concentration of 50 µg/mL, the calibration solutions with concentrations of 25, 15, 12, 10, 8, 6, 4, 2, 1 and 0.5 µg/mL were set.

Calibration solutions were filtered with 0.22 µm filters and analyzed by RP-HPLC.

5. Determination of Minimum Inhibitory Concentrations for Daptomycin

Determination of Minimum Inhibitory Concentration (MIC) was executed following standards for antimicrobial susceptibility testing, provided by Clinical and Laboratory Standards Institute (CSLI) in documents M7-A6 and M100-S15, and the procedure for susceptibility testing of daptomycin by broth microdilution method, provided by Novartis®. Both guidelines recommend the use of Broth Microdilution Method.

Assays were performed in 96-well microplates, allowing to compare the MIC of free daptomycin with the MIC of entrapped daptomycin, at concentrations of 0.03, 0.06, 0.12, 0.25, 0.5, 1.0, 2.0, 4.0, 8.0 and 16.0 µg/ mL, against the following organisms: methicillin-susceptible *Staphylococcus aureus* ATCC 25913 (MSSA), methicillin-resistant *Staphylococcus aureus* ATCC 43300 (MRSA), *Staphylococcus epidermidis* ATCC 14990, *Staphylococcus capitis* ATCC 27840, *Staphylococcus hominis* ATCC 13348, *Staphylococcus lugdunensis* ATCC 43809, *Staphylococcus haemolyticus* ATCC 29970 and *Staphylococcus warmeri* ATCC 13354.

First, it was performed a calcium adjustment of Mueller-Hinton broth to a final concentration of 50 mg/ L Ca^{2+}, using a calcium stock solution. Inocula were prepared by suspending each bacteria colony into the calcium adjusted Mueller-Hinton broth, achieving a turbidity equivalent to 0.5 McFarland standard ($1x10^8$ CFU/ mL), and then diluted in the calcium adjusted Mueller- Hinton, to reach the recommended concentration of bacteria in wells, 5×10^5 CFU/ mL.

Fitfty microliters L of each inoculum were transferred to the microplate and every well was fulfilled with free daptomycin or daptomycin-loaded nanoparticles at concentrations cited above.

Further on, three controls were also done at the same time: the first one containing inoculum and Mueller-Hinton broth, the second one containing only daptomycin (free or entrapped) and the third one containing Mueller-Hinton broth.

6. Determination of the permeability of daptomycin in ocular cells

The drug permeability prediction across the ocular tissues is important in the development of new drugs and drug delivery strategies. It is known that cornea is the major absorption route for topically applied drugs and corneal epithelium represents the rate-limiting barrier for transcorneal permeation (Hornof *et al.*, 2005; Barar *et al.*, 2009). In this experiment, permeability of daptomycin in corneal and blood-retinal epitheliums was tested using cell culture models.

Assays for determination of daptomycin permeability in ocular cells were realized for ARPE – 19 (human retinal pigment) and HCE (human corneal epithelium) epithelial cell lines, which are widely used in cell culture models, as they both have the structural and functional properties of retinal epithelium and corneal epithelium *in vivo*, respectively (Dunn *et al.*, 1996; Barar *et*

al., 2009). This experiment was performed following the method used by Geiger and co-workers (Geiger *et al*., 2005), with slight modifications.

6.1. Cell culturing

Human adult ARPE-19 and HCE cells were grown in DMEM supplemented with 10% fetal bovine serum (FBS), 1% penicillin-streptomycin and 1% amino acids mixture, on tissue culture-treated T-25 and T-75 flasks, at 37ºC. Medium was substituted every 2 – 3 days, until confluence was achieved.

6.2. Cell seeding

Cells were then plated on 6-well tissue culture test plates provided with PET membranes inserts: for each cell line, medium was aspired, cells were washed with PBS, incubated with trypsin for 5 minutes at 37ºC and DMEM was added again. For each well, it was passed 2.5 mL of DMEM, Transwell® inserts were then collocated and 1.5 mL of DMEM and cells were added, 120.000 for ARPE-19 cells and 100.000 for HCE cells. Figure 2.1 presents, schematically, the *in vitro* cell culture mode.

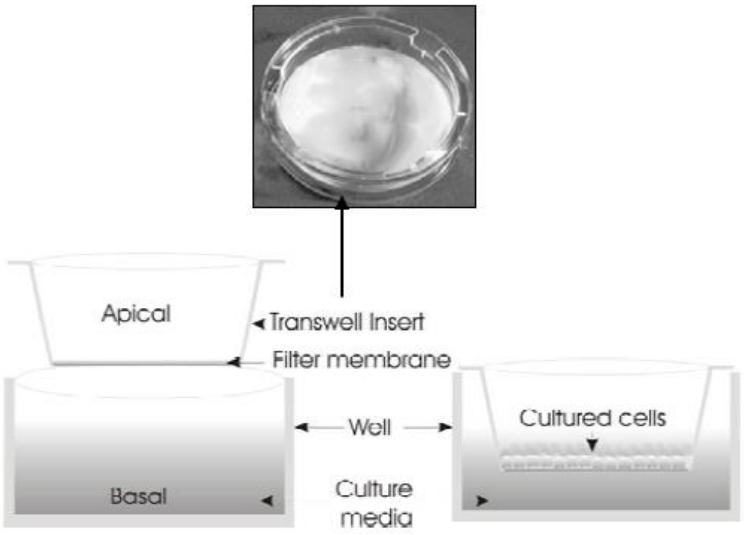

Figure 2.1 – Schematic representation of the in vitro cell culture model, using transwell inserts (Barar *et al*., 2009).

Medium was replaced once a week (2.5 and 1.5 mL from basolateral and apical compartments, respectively) and transepithelial resistance (TER) was measured with a

voltmeter, until 80-110 mΩ value was achieved. The final concentration of cells in each well was 200.000 cell/ cm^2 for ARPE-19 cell line, and 90.000 cell/cm^2 for HCE cell line.

6.3. Permeability Experiment

Thirty minutes before start of the experiment, cells were rinsed with complete HBSS (2.5 mL basolaterally and 1.5 mL apically). At the start of the experiment, the complete volume of HBSS was removed and replaced with new HBSS, with the respective volumes. Daptomycin in free and encapsulated forms was added to apical compartment.

Permeability measurements were made at 15, 30, 60, 120,180 and 240 minutes, removing 100 µL aliquots from basolateral compartment and adding 100 µL of HBSS to the same compartment. Removed aliquots were then measured for daptomycin concentration using RP-HPLC.

7. Statistical Analysis

Obtained results were statistical analyzed with IBM SPSS Statistics 19, using Linear Regression, T-student for paired samples and One-Way Analysis of Variance (ANOVA) with Tukey HSD post-hoc test. The differences were considered significant at a level of 95% ($p < 0.05$).

III. Results and Discussion

The main purpose of this work was the development of an effective daptomycin carrier system that could be used to deliver this novel antibiotic directly into the eye. Chitosan coated alginate nanoparticles were selected for this purpose, due to chemical and biological properties of alginate and chitosan, such as biocompatibility, biodegradability, mucoadhesiveness and non-toxicity, as described previously. Nanoparticles are colloidal carrier systems that can improve the efficacy of drug delivery by overcoming diffusion barriers, permitting reduced dosing as well as sustained delivery and appear to be the most promising tool to meet the primary requirements of and ideal ocular delivery system (Zarbin *et al*., 2010; Liu *et al*., 2012).

In order to achieve an efficient antibiotic delivery system into the eye that would be able to treat bacterial endophthalmitis, it was prepared chitosan coated alginate nanoparticles for incorporation of daptomycin. As previously described, alginate-chitosan nanoparticles are also biocompatible, biodegradable, non-toxic, and capable to sustain the release of encapsulated materials more efficiently than either alginate or chitosan alone, which represents the major advantage for using chitosan coated sodium alginate nanoparticles (Motwani *et al*., 2007; Nagarwal *et al*., 2012).

1. Characterization of chitosan coated sodium alginate nanoparticles

Nanoparticles were produced by ionotropic gelation of alginate with calcium counter ions, followed by polyelectrolyte complex coating with chitosan.

Ionotropic gelation is based on the capability of electrolytes to cross link in the presence of counter ions to form hydrogels. Alginate is soluble in water and forms a reticulated structure which can be cross-linked with divalent or polyvalent cations to form insoluble meshwork, i.e. calcium and zinc cations that have been reported for cross-linking of acid groups of alginate (Patil *et al*., 2010). The quality of hydrogel beads prepared by ionotropic gelation method can also be further improved by polyelectrolyte complexation technique: the negatively charged carboxylic groups of acid units in alginate interact electrostatically with the positively charged amino groups in chitosan to form a polyelectrolyte complex (Patil *et al*., 2010; Hamman, 2010). This polyelectrolyte complex acquires great interest as it is still biodegradable and

biocompatible and yet is mechanically stronger at lower pH values, where chitosan dissolves (Hamman, 2010).

Silva (Silva *et al*., 2013) demonstrated that the isoelectric point of daptomycin is between 4.3 and 4.4, below these pH values it is positively charged and above these pH values it is negatively charged. Sodium alginate is negatively charged and chitosan is positively charged (Harnsilawat *et al*., 2006; Chen *et al*., 2009; Nagpal *et al*., 2010). Considering these characteristics, pH of all solutions was adjusted to 3.5 – 3.6, in order to allow attractive electrostatic interactions between them.

1.1. Unloaded nanoparticles

Chitosan coated alginate unloaded nanoparticles were previously prepared in order to evaluate the effect of different concentrations of alginate, chitosan and calcium chloride in physicochemical characteristics of nanoparticles and also to determine the best mass ratio between alginate and chitosan to encapsulate daptomycin.

The physicochemical characteristics of the nanoparticles obtained were analyzed for particle size, polydispersity index and Zeta potential by photo correlation spectroscopy and laser Doppler anemometry.

The results of the first set of nanoparticles are presented in table 3.1 (corresponding to the formulations presented on table 2.1), which shows that major of formulations originated nanoparticles, although formulations using larger concentrations of sodium alginate (0.71 and 0.95 mg/ mL) do not allow nanoparticle formation but originated aggregates instead.

It is possible to observe that nanoparticles obtained have sizes between 502.8 ± 7.8 and 1088.3 ± 25.6 nm, with smallest particles (502.8 and 504.2 nm) being produced with a higher mass ratio between alginate and chitosan, which was is 1: 0.07. It is known that particle size for ophthalmologic applications should not exceed 10 µm, because with larger sizes a scratching feeling might occur, so it is important to reduce the particle size in order to improve the patient comfort during administration (Zimmer and Kreuter, 1995). Statistical analysis showed that there are significant differences ($p = 0.025$) between the sizes of nanoparticles prepared with different concentrations of alginate, which indicates that particle size also depends on alginate concentration and not only on mass ratio. However, there is no relation between chitosan concentration and particles size ($p > 0.05$).

Table 3.1 - Particle size, polydispersity and zeta potential of preliminary experiment for unloaded chitosan coated alginate nanoparticles.

Alginate Concentration* (mg/mL)	Chitosan Concentration* (mg/mL)	$CaCl_2$ Concentration* (mg/mL)	Alginate: Chitosan mass ratio	Particle size (nm)	Polydispersity	Zeta Potetial (mV)
0.24	0.08	0.11	1: 0.07	502.8 ± 7.8	0.221 ± 0.006	-26.61 ± 0.64
0.48	0.04	0.11	1: 0.018	1007.3 ± 26.8	0.347 ± 0.009	- 47.70 ± 0.94
	0.08	0.06	1: 0.035	1088.3 ± 25.6	0.380 ± 0.010	-55.85 ± 0.82
		0.11	1: 0.035	740.6 ± 28.7	0.361 ± 0.009	- 46.50 ± 0.63
	0.17	0.11	1: 0.07	504.2 ± 6.6	0.315 ± 0.006	- 44.70 ± 0.87
0.71	0.08	0.11	1 : 0.024		Aggregates	
0.95	0.08	0.11	1 : 0.018		Aggregates	

* Concentration on final solution. Data shown are the mean ±standard deviation (n=3).

The effect of different $CaCl_2$ concentrations was not fully tested, however it is possible to observe that for nanoparticles produced with the same amounts of alginate and chitosan (0.48 and 0.08 mg/ mL, respectively), the nanoparticles size was smaller for those prepared with higher $CaCl_2 \cdot 2H_2O$ concentration (0.11 mg/ mL).

The polydispersity has a range between 0.221 and 0.380 and does not seem to have a relationship with the used mass ratio between alginate and chitosan, however the lower value was achieved when the alginate concentration was reduced (0.24 mg/ mL). In fact, polydispersity revealed to be dependent on alginate concentration ($p = 0.000$) but it does not vary with chitosan concentration ($p > 0.05$).

Zeta potential is the measure of the charge that develops at the interface between a solid surface and its liquid medium, representing an index for particle stability. As the zeta potential increases, the repulsive interactions will be larger leading to the formation of more stable particles with a size distribution more uniform (Hans and Lowman, 2002).

The zeta potential of analyzed nanoparticles is negative due to alginate higher concentrations and has an absolute value above 40 mV in most cases. Hans and Lowman (2002) suggested that a physically stable nanosuspension solely stabilized by electrostatic repulsion if have a minimum zeta potential of ± 30 mV, so it is reasonable to conclude that the produced nanoparticles are stable. It is also possible to observe that nanoparticles with lower

concentration of alginate achieved the lowest zeta potential absolute value (-26.61 mV), however it does not seem to have relation with the mass ratio between alginate and chitosan. In fact, statistical analysis showed that there are significant differences (p=0.000) between nanoparticles with different alginate concentrations.

From this experiment it can be concluded that alginate and chitosan are suitable for production of eye drug delivery nanoparticles, although it depends on alginate, chitosan and $CaCl_2$ concentrations and the mass ratio between alginate and chitosan. Furthermore, nanoparticles with smaller sizes were obtained with greater mass ratios, which suggests that it is possible to obtain smaller nanoparticles prepared with reduced concentrations of alginate and larger concentrations of chitosan.

After these preliminary results, it was set a new experiment using the same method but using lower concentrations of alginate and higher mass ratios. Table 3.2 presents the obtained results.

For this experiment it was used a single reduced alginate concentration, relating to the former experiment, which allowed a greater mass ratio between alginate and chitosan. Chitosan concentrations used were 0.02, 0.05 and 0.08 mg/ mL to permit some range of mass ratio without exceeding alginate concentration. The mass ratios obtained were 1:0.05, 1:0.14 and 1:0.22. It was also used different concentrations of $CaCl_2$ to observe if there was any relation between concentration of calcium chloride and the characteristics of nanoparticles.

Table 3.2 shows that for 1:0.05 and 1:0.14 mass ratios between alginate and chitosan, it was obtained nanoparticles with sizes between 301.8 and 398.3 nm. These nanoparticles are smaller than nanoparticles obtained in the previous experiment, though there are not statistically differences between them ($p > 0.05$). However, contrary to what was expected, a mass ratio of 1:0.22 between alginate and chitosan has led to the formation of larger nanoparticles, with sizes among 715.8 and 877.0 nm. In fact, statistical analysis permits to observe that there are significant differences ($p = 0.000$) between nanoparticles with a mass ratio of 1: 0.22 and all the others, which can be related to chitosan concentration, as nanoparticles prepared with a concentration 0.08 mg/ mL of chitosan presented larger particle sizes. This result suggests that using reduced concentrations of alginate allows the formation of smaller nanoparticles, yet the concentration of chitosan must be less than the concentration of alginate. These results are in accordance with the results previously reported by Sarmento and colleagues (Sarmento *et al*., 2007), who obtained alginate and chitosan unloaded nanoparticles with 781 ± 61 nm.

Regarding to polydispersity, nanoparticles presented values between 0.197 and 0.242 when chitosan concentration is 0.02 mg/ mL, values between 0.249 and 0.281 for a chitosan concentration of 0.05 mg/ mL and values above 0.360 for a chitosan concentration of 0.08 mg/ mL. Nanoparticles with a mass ratio of 1:0.05 have less polydispersity than nanoparticles with a mass ratio of 1:0.14 ($p = 0.02$) and both present lower value of polydispersity than nanoparticles with a mass ratio of 1:0.22 ($p = 0.000$). It can be concluded that formulations that had led to smaller sizes of nanoparticles also led to nanoparticles with lower polydispersity.

Table 3.2 - Particle size, polydispersity and zeta potential of unloaded chitosan coated alginate nanoparticles, after preliminary study.

Alginate Concentration* (mg/mL)	Chitosan Concentration* (mg/mL)	$CaCl_2$ Concentration* (mg/mL)	Alginate: Chitosan mass ratio	Particle size (nm)	Polydispersity	Zeta Potetial (mV)
0.08	0.02	0.04	1: 0.05	313.8 ± 81.8	0.242 ± 0.005	-38.22 ± 0.29
		0.06		398.3 ± 25.5	0.197 ± 0.007	- 38.50 ± 0.14
		0.08		349.9 ± 38.2	0.236 ± 0.004	-38.43 ± 0.17
	0.05	0.04	1: 0.14	394.9 ± 17.3	0.279 ± 0.009	-38.45 ± 0.11
		0.06		394.0 ± 4.3	0.249 ± 0.013	- 38.39 ± 0.13
		0.08		301.8 ± 17.9	0.281 ± 0.014	- 38.29 ± 0.07
	0.08	0.04	1: 0.22	715.8±139.0	0.366 ± 0.006	- 38.29 ± 0.14
		0.06		877.0 ± 32.8	0.367 ± 0.011	- 38.44 ± 0.04
		0.08		816.3±138.2	0.370 ± 0.004	- 38.35 ± 0.14

* Concentration on final solution. Data shown are the mean ±standard deviation (n=3).

Zeta Potential is ca. -38 mV for all formulations and there are no statistical differences ($p > 0.05$) between them, which suggests that zeta potential is mainly affected by alginate concentration and a 0.08 mg/ mL alginate concentration allows the formation of physically stable nanoparticles.

Considering the low particle size and polydispersity achieved, it was selected the formulation with concentrations of 0.08 mg / mL of alginate, 0.02 mg/ mL of chitosan and 0.04 mg/mL of calcium chloride to create daptomycin loaded nanoparticles.

1.2. Daptomycin loaded nanoparticles

Daptomycin-loaded chitosan coated alginate nanoparticles were prepared following the same procedure as unloaded nanoparticles. The concentrations of alginate, chitosan and calcium chloride used were 0.08, 0.02 and 0.04 mg/ mL, respectively, and daptomycin concentrations ranged between 10 and 330 µg/ mL, as detailed on Table 2.3.

The characterization of daptomycin loaded nanoparticles obtained is presented on Table 3.3.

Table 3.3 – Particle size, polydispersity and zeta potential for daptomycin loaded chitosan coated alginate nanoparticles, prepared at different alginate: daptomycin mass ratios.

Daptomycin concentration* (µg/ mL)	Alg : dapto mass ratio	Particle Size	Polydispersity	Zeta Potential
10	1 : 0.01	393.0 ± 31.3	0.201 ± 0.003	-25.18 ± 0.64
20	1: 0.03	382.8 ± 7.5	0.171 ± 0.030	-23.48 ± 0.20
40	1: 0.05	407.1 ± 77. 3	0.186 ± 0.046	-19.69 ± 1.34
80	1 : 0.1	421.2 ± 55.1	0.231 ± 0.036	-24.48 ± 0.17
160	1 : 0.2		Aggregates	
330	1 : 0.4		Aggregates	

* Concentration on final solution. Data shown are the mean ±standard deviation (n=3).

It is possible to observe that formation of nanoparticles is only possible for some daptomycin concentrations, as for concentrations of daptomycin above 80 µg/mL aggregates were formed and quickly precipitated. Nanoparticles were formed with sizes between 382.8 ± 7.5 and 421.2 ± 55.1 nm, polydispersity between 0.171 ± 0.030 and 0.231 ± 0.036 and zeta potential between -19.69 ± 1.34 and -25.18 ± 0.64 mV.

Daptomycin loaded nanoparticles achieved have a slightly larger size than unloaded particles with same amounts of alginate and chitosan from previous experiment (313.8 ± 81.8 nm) and there are no significant differences ($p > 0.05$) in particle size among the different concentrations of daptomycin that was used.

Unlike the particle sizes, polydispersity seems to have lower values, when compared to unloaded nanoparticles with same formulation. However, there is no correlation with daptomycin concentration used as there are no statistically significant differences between formulations ($p > 0.05$).

Zeta potential was negative, as expected, with values between -25.18 ± 0.64 and -19.69 ± 1.34. Nevertheless, zeta potential values of daptomycin loaded nanoparticles are lower that zeta potential values of unloaded nanoparticles (ca. -38 mV), which can be explained by the lower concentration of alginate and, thereafter, less negative charges. Absolute values are below 30 mV, which indicates that obtained daptomycin loaded nanoparticles are not very stable. There are not significant differences ($p > 0.05$) for zeta potential values obtained, except for nanoparticles prepared with 40 µg/mL, which zeta potential value is statistical lower ($p = 0.001$), however in the same range, and with no apparent reason to justify significant difference.

2. Determination of encapsulation efficiency of daptomycin- loaded nanoparticles

The determination of daptomycin encapsulation efficiency into chitosan coated sodium alginate nanoparticles was established by estimating the amount of free drug in the supernatant after centrifugation of nanoparticle suspensions by RP-HPLC. Therefore, daptomycin encapsulation efficiency was calculated as the percentage of drug entrapped in alginate nanoparticles compared with the initial amount of drug.

Table 3.4 presents the results of daptomycin loaded nanoparticles encapsulation efficiency. The highest encapsulation efficiency achieved was 91.45 ± 0.69%, for a daptomycin concentration of 10 µg/ mL, followed 20 µg/ mL of daptomycin-loaded nanoparticles, for which encapsulation efficiency was 88.90 ± 9.49 %. Formulations with daptomycin concentrations of 40 µg/ mL and 80 µg/ mL had medium encapsulation efficiencies, and 78.75 ± 31.38 %, and 78.93 ± 3.51%, respectively.

Statistically, there are not significant differences among encapsulation efficiency of different nanoparticles ($p > 0.05$) and is not possible to obtain a linear regression between daptomycin concentration or alginate/ daptomycin mass ratio and encapsulation efficiency ($r = 0,597$).

Table 3.4 – Encapsulation efficiency of daptomycin loaded chitosan coated alginate nanoparticles, at different alginate: daptomycin mass ratios.

Daptomycin Concentration (µg/ mL)	Alginate : Daptomycin mass ratio	Encapsulation Efficiency (%)
10	1 : 0.01	91.45 ± 0.69
20	1: 0.03	88.90 ± 9.49
40	1: 0.05	78.75 ± 20.38
80	1 : 0.1	78.93 ± 3.51

* Concentration on final solution. Data shown are the mean ±standard deviation (n= 3).

Encapsulation efficiency for daptomycin concentration at 40 µg/mL has a high standard deviation value, which may be related to zeta potential. Zeta potential absolute value for loaded nanoparticles was 19.69 mV (Table 3.3), indicating that nanoparticles were not very stable and did not allow an extended electrostatic interaction between alginate and daptomycin for some samples.

Having a general glance at the results, it is possible to observe that encapsulation efficiency was in accordance with results obtained by other authors who used chitosan coated alginate nanoparticles for encapsulation of other drugs. Sarmento and colleagues (Sarmento *et al.*, 2007) obtained an insulin encapsulation efficiency of 73% and Zahoor and colleagues (Zahoor *et al.*, 2005) obtained encapsulation efficiencies for rifampicin of 80 – 90%. On the other hand, Nagarwal and colleagues (Nagarwal *et al.*, 2012) obtained an encapsulation efficiency of 6.2 – 26.7% for 5 – Fluorouracil with the purpose of ocular delivery, although 5-FU is an antiviral drug.

3. Minimum Inhibitory Concentrations

Determination of MIC was performed for free and nanoparticle-entrapped daptomycin, and executed by Broth Microdillution Method. The calcium concentration of Mueller-Hinton broth was adjusted to 50 mg/ L, once daptomycin requires the presence of physiologic levels of calcium ions for the most accurate expression of its antibiotic activity. MIC corresponds to the lowest concentration of the agent tested that inhibits visible bacterial growth, by absence of turbidity when compared to a control (Silva *et al.*, 2013)

Daptomycin loaded nanoparticles were prepared in order to contain the same amount of daptomycin presented in daptomycin solution, based on encapsulation efficiencies previously determined.

Table 3.5 presents the obtained MIC for the tested microorganisms, allowing to compare MIC for daptomycin solution with MIC for daptomycin loaded nanoparticles.

Table 3.5 – Minimum Inhibitory Concentrations for free daptomycin and daptomycin-loaded nanoparticles against eight selected microorganisms.

	MIC (µg/ mL)	
Microrganism	**Daptomycin Solution***	**Daptomycin loaded nanoparticles***
MSSA	0.5	0.5
MRSA	1	1
S. epidermidis	0.5	0.5
S. capitis	1	0.5
S. hominis	0.25	0.25
S. lugdunensis	2	2
S. haemolyticus	0.5	0.5
S. warmeri	0.25	0.5

* n = 2.

MIC values for daptomycin in both forms (free and entrapped) vary between 0.25 and 1 µg/ mL, except for *S. lugdunensis*, indicating that all microorganisms were susceptible to

daptomycin at concentrations below the susceptibility breakpoint established for staphylococci (≤1 μg/ mL) by the European Committee on Antimicrobial Susceptibility Testing.

MIC values obtained for free daptomycin for MRSA (0.5 μg/ mL), MSSA (1 μg/ mL), S. *epidermidis* (0.5 μg/ mL) and S. *haemolyticus* (0.5 μg/ mL) are in agreement with the MIC range reviewed in literature: < 0.06 – 2 μg/ mL (Fuchs et al., 2002; Barry et al., 2001), 0.06 – 2 μg/ mL (Fuchs et al., 2002; Barry et al., 2001), 0.06 – 0.5 μg/ mL (Fluit et al., 2004) and 0.25 – 0.5 μg/ mL (Fuchs et al., 2002), respectively.

Although MIC value for *S. capitis* was lower for daptomycin-loaded nanoparticles than for free daptomycin and *S. warmeri* presented lower MIC value in free form than in entrapped form, there are no statistical significant differences ($p > 0.05$) between obtained MIC for free daptomycin and MIC for daptomycin-loaded nanoparticles.

The fact that there are no differences between MIC values for daptomycin in solution or loaded nanoparticles suggests that widely known antimicrobial activity of chitosan did not interfere in the experiment. On one hand, the concentration of chitosan used to prepare nanoparticles was low (0.02 mg/ mL) and, on the other hand reported MIC values for chitosan are higher than 16 μg/ mL. For instance, Tanjak and co-workers (Tanjak *et al*., 2011) determined MIC for chitosan against some bacteria: 1000 μg/ mL for *S. epidermidis* and 512 μg/ mL for *S. aureus*.

In conclusion, all microorganisms were susceptible to daptomycin, with MIC values below 2 μg/ mL. Daptomycin maintains antibiotic properties in solution form and nanoparticle form, suggesting that the use of nanoparticles for daptomycin delivery into the eye will not affect its antimicrobial efficiency.

4. Determination of the permeability of daptomycin in ocular cells

It is of vital importance for the eye to maintain a highly regulated environment for the visual cells and transparent tissues. Consequently, tight cellular barriers, which restrict and regulate the uptake of fluids and solutes, are present in the anterior and posterior parts of the eye. These barriers are fundamentally important for the protection of the eye and for the maintenance of vital ocular functions. Ocular barriers effectively protect the eye also from pharmaceuticals (Hornof *et al*., 2005). Many diseases of the retina are characterized by permeability increases

in the blood-retinal barrier. Through the formation of tight junctions, the retinal endothelial cells and the retinal pigmented epithelium form an almost impermeable boundary that can prevent molecules as small as ions from crossing this barrier (Geiger *et al*., 2005).

The drug permeability prediction across the ocular tissues is important in the development of new drugs and drug delivery strategies. In this experiment, permeability of daptomycin in corneal and blood-retinal epitheliums was tested using cell culture models. It is known that cornea is the major absorption route for topically applied drugs, even though it forms a tight barrier, and corneal epithelium represents the rate-limiting barrier for transcorneal permeation, providing over 60% of total corneal resistance (Hornof *et al.*, 2005; Barar *et al*., 2009). Blood-retinal barrier forms a strong barrier because of its tight junctions, as previously described.

HCE and ARPE-19 cell lines were used as *in vitro* models of corneal and blood-retinal epitheliums, respectively, to determine permeability of daptomycin in these tissues. Immortalized corneal epithelial cell lines established from rabbit, rat, hamster, and humans, immortalized human cell lines (e. g., HCE) are widely used in cell culture models (Barar *et al.*, 2009). ARPE-19 cell line was characterized by Dunn *et al*. (Dunn *et al*., 1996), who concluded that this human RPE cell line has structural and functional properties characteristic of RPE cells *in vivo*.

In vitro cell culture model used Transwell® inserts, a permeable support system that allows assessment of bioelectrical and permeability properties of cell cultures (Barar *et al*., 2009). Permeability of free daptomycin and encapsulated daptomycin, i.e., percentage of initial amount of daptomycin that crosses cellular layers, was measured at 15, 30, 60, 120, 180 and 240 minutes. Results comparing permeability of daptomycin in different forms are presented in graphics 3.1 and 3.2, for HCE and ARPE-19 cells, respectively.

In Figure 3.1, it is possible to compare permeability of daptomycin solution and daptomycin-loaded chitosan coated alginate nanoparticles in HCE cells. Data shown are the mean ±standard deviation (n=3).

Data shows that permeability in HCE cells ranges 3.76 to 18.76% for daptomycin solution, and 0.41 to 6.37% for daptomycin-loaded nanoparticles, and statistical analysis revealed that these differences are statistically significant ($p = 0.000$).

It is evident that permeability in HCE cell for daptomycin in solution form is higher, however it is important to remember that, in this experiment, daptomycin was directly put in contact with

the HCE layer so 100% of the antibiotic contacted with corneal epithelium. *In vivo*, topical administration of daptomycin would not be so successful, once cornea is negatively charged and so is daptomycin.

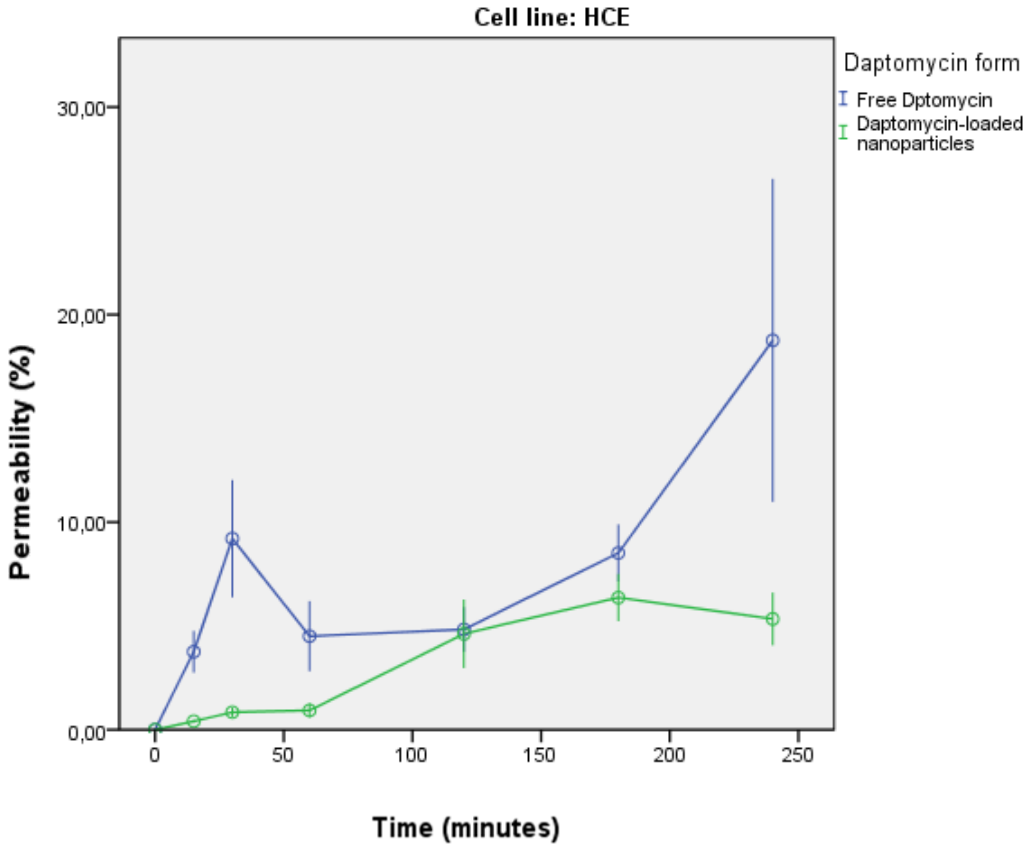

Figure 3.1 - Permeability in HCE cells for daptomycin solution and daptomycin-loaded nanoparticles. Data shown are the mean ±standard deviation (n=3).

Even the permeability for daptomycin-loaded nanoparticles being lower, chitosan coated alginate nanoparticles could be a useful tool to overcome the lack of mucoadhsiveness and short residence time of drug in corneal epithelium.

In Figure 3.2, it is possible to compare permeability in ARPE-19 cells for daptomycin solution and daptomycin-loaded chitosan coated alginate nanoparticles. Data shown are the mean ±standard deviation (n=3).

First of all, permeability of free daptomycin varies from 2.2 to 12.2% while permeability in daptomycin-loaded nanoparticles ranges from 1.0 to 5.0%, between 15 and 240 minutes after drug application, in ARPE-19 cells. These differences are statistically significant ($p = 0.000$),

indicating that permeability in ARPE-19 cells is higher for daptomycin solution than for daptomycin loaded nanoparticles.

Similar to HCE cells, also permeability in ARPE-19 cells was higher for daptomycin in solution form than in encapsulated form. However, it is possible to observe that after 240 minutes, the amount of daptomycin (in both solution and nanoparticle form) that penetrated HCE cells layer was higher than the amount of antibiotic that had crossed ARPE-19 cells layer, suggesting a greater resistance from retinal epithelium to daptomycin.

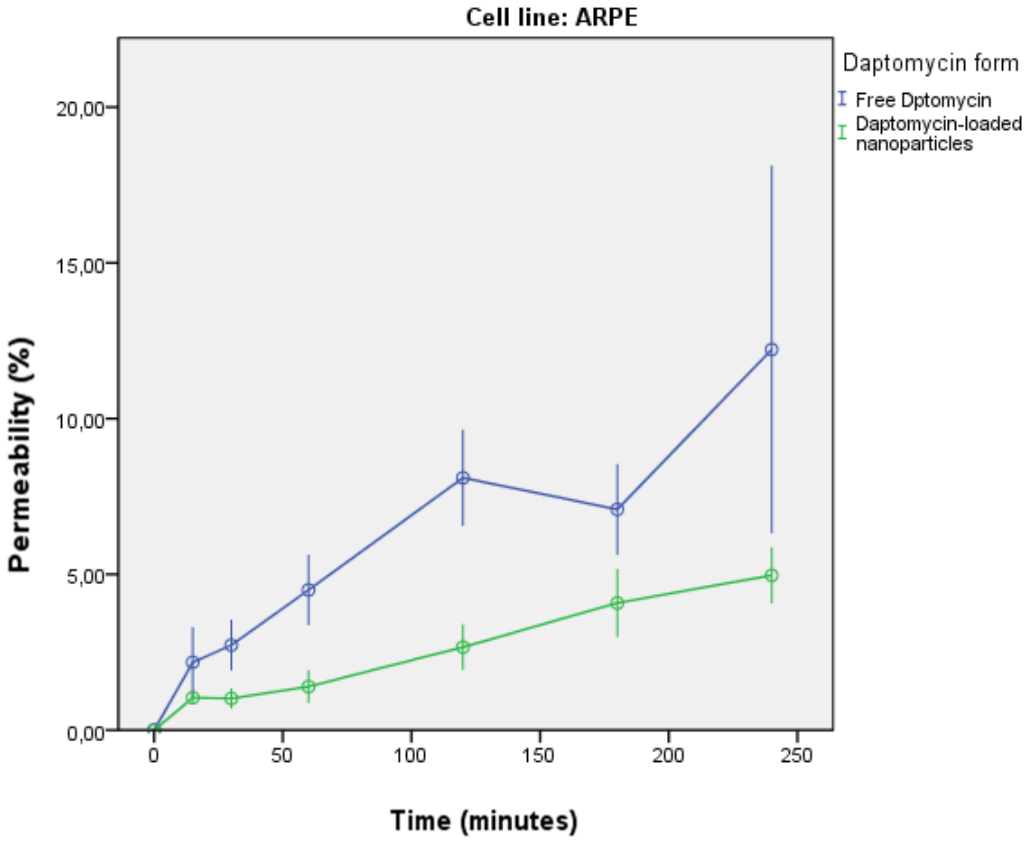

Figure 3.2 – Permeability in ARPE-19 cells for daptomycin solution and daptomycin-loaded nanoparticles. Data shown are the mean ±standard deviation (n=3).

It is important to recall that human eyeball is constituted by several layers, with different histological properties so, in the case of topical administration, there would be previous drug loss before retinal epithelium penetration, suggesting that developed antibiotic nanocarries should be more mucoadhesive, in order to prolong drug contact time with the eyeball and increase the released amount of daptomycin in the posterior segment of the eye, where bacterial endophthalmitis occur.

Finally, the slower penetration of encapsulated daptomycin into both cell layers suggests that this drug delivery system could constitute a controlled drug delivery system, releasing small amounts of drug for a few hours.

IV. Conclusions

The main purpose of this research work was the development of an effective daptomycin nanocarrier system that could be used to deliver this novel antibiotic directly into the eye, in order to act as a prospective therapy against Bacterial Endophthalmitis and as an efficient alternative to chitosan nanoparticles.

Daptomycin has been proven to be a powerful antimicrobial agent against a wide range of microorganisms responsible for eye infections, namely *Streptococcus aureus* and Methicillin-resistant *Streptococcus aureus*, which are no longer susceptible to main antibiotics as Vancomycin.

Because of daptomycin negative charges, topical administration of this antibiotic into the eye is not possible as cornea and conjunctiva are also negatively charged, the use of mucoadhesive polymers to carry daptomycin directly into the eye constitute an interesting way to treat endophthalmitis.

Sodium alginate constitutes a promising material for development of drug topical delivery systems due to its biological and chemical properties as biodegradability, non-toxicity, biocompatibility and mucoadhesiveness. However, alginate surface charge is also negative, preventing it from binding to ocular layers, so coating sodium alginate nanoparticles into chitosan allows to overcome the mucoadhsiveness problem.

Formulated daptomycin-loaded chitosan coated sodium alginate nanoparticles were characterized for their physicochemical properties and revealed to have sizes between 382.8 ± 7.45 and 421.2 ± 55.12 nm, suitable for ocular applications. Zeta potential values of developed nanoparticles confirm their physical stability. Encapsulation efficiency of daptomycin into these nanoparticles ranged between 78.93 ± 3.51 and 91.45 ± 0.69%, allowing to admit that there is a diminutive waste of the antibiotic.

Antibacterial activity of daptomycin against major microorganisms responsible for bacterial endophthalmithis was not affected and both daptomycin solution and daptomycin-loaded nanoparticles revealed to have the same powerful antibacterial activity.

In vitro ocular permeability to daptomycin-loaded nanoparticles was tested using cell culture models for corneal and retinal epithelium and it were obtained permeabilities ranging from 0.41 to 6.37% for corneal cells and 1.04 to 4.97% for retinal cells between 15 minutes and 4 hours,

suggesting that this drug delivery system could constitute a controlled drug delivery system, releasing small amounts of drug for a few hours.

Comparing to results obtained by Silva *et al*. (2013) for daptomycin-loaded chitosan nanoparticles, alginate-chitosan nanoparticles revealed to have larger sizes but similar polidispersity indexes and zeta potential absolute values. Encapsulation efficiencies were similar, ranging 80-90% in both cases. However, for some chitosan nanoparticles developed by the same author (Silva *et al*., 2013), minimum inhibitory concentrations of daptomycin against some microorganisms were higher after encapsulation into chitosan nanoparticles, which was not verified for alginate-chitosan nanoparticles. Besides these differences, the major advantage for the use of alginate-chitosan nanoparticles is to improve the sustained release, which should be tested in the future.

To sum up, developed chitosan coated sodium alginate daptomycin loaded nanoparticles seem to be an interesting and potential therapy for bacterial endophthalmitis treatment and more research work is required in order to achieve this final goal.

This work constitutes an important preliminary study and can be completed in the future by studying more biological and pharmaceutical properties of developed nanoparticles, including: *in vitro* cytotoxic testing, sustained release testing, evaluation of nanoparticles stability when in contact with ocular fluids, namely tear film, and retain the long-term stability of developed nanoparticles after freeze-drying and sterilization.

V. References

Alonso, M. J., Sánchez, A. 2003. The potential of chitosan in ocular drug delivery. *Journal of Pharmacy and Pharmacology* **55**: 1451-1463.

Barar, J., Asadi, M., Mortazavi-Tabatabaei, S., Omidi, Y. 2009. Ocular drug delivery; impacto of in vitro cell culture models. *Journal of Ophthalmic and Vision Research* **4** (4): 238 – 252.

Barry, A. L., Fuchs, P. C., Brown, S. D. 2001. In vitro activities of daptomycin against 2,798 clinical isolates from 11 North American medical centers. *Antimicrobial Agents and Chemotherapy* **45** (6): 1919 – 1922.

Benz, M. S., Scott I. U., Flynn Jr., H. W., Unonius, N., Miller, D., 2004. Endophthalmitis isolates and antibiotic sensitivities: a 6 year review of cultures-proven cases. *American Journal of Ophthalmology* **137** (1): 38-42.

Bochot, A., Couvreur, P., Fattal, E. 2000. Intravitreal administration of antisense oligonucleotides: potential of liposomal delivery. *Progress in Retinal and Eye Research* **19**: 131 – 147.

Callegan, M. C., Engelbert, M., Parke II, D. W., Jett, B. D., Gilmore, M. S. 2002. Bacterial endophthalmitis: Epidemiology, Therapeutics, and Bacterium-Host Interactions. *Clinical Microbiology Reviews* **15** (1): 111-124,

Callegan, M. C., Gilmore, M. S., Gregory, M., Ramadan, R. T., Wiskur, B. J., Moyer, A. L., Hunt, J. J., Novosad, B. D. 2007. Bacterial endophthalmitis: Therapeutic challenges and host-pathogen interactions. *Progress in Retinal and Eye Research* **26**: 189-203.

Chen, A., Haddad, D., Wang, R. 2009. Analysis of Chitosan - Alginate Bone Scaffolds. Rutgers University: New York

Clinical and Laboratory Standards Institute. 2003. Methods for dilution antimicrobial susceptibility test for bacteria that grow aerobically, NCCLS document M7-A6, 6th edition. Villanova, Pennsylvania, USA.

Clinical and Laboratory Standards Institute. 2005. Performance Standards for antimicrobial susceptibility testing, 15th informational supplement, NCCLS document M100-S15. Villanova, Pennsylvania, USA.

Drake, R. L., Vogl, A. W., Mitchell, A. W. M. 2010. Gray's Anatomy for Students, 2nd Edition. Churchill Livingstone, Philadelphia, pp. 899-901.

Dunn, K. C., Aotaki-Keen, A. E., Putkey, F. R., Hjelmeland, L. M. 1995. ARPE-19, a human retinal pigment epithelial cell line with differentiated properties. *Experimental Eye Research* **62**: 155 – 169.

De Campos, A. M., Diebold, Y., Carvalho, E. L. S., Sánchez, A., Alonso, M. J. 2004. Chitosan nanoparticles as new ocular drug delivery systems: *in vitro* stability, *in vivo* fate, and cellular toxicity. *Pharmaceutical Research* **21** (5): 803-810.

De la Fuente, M., Raviña, M., Paolicelli, P., Sanchez, A., Seijo, B., Alonso, M. J. 2010. Chitosan-based nanostructures: a delivery platform for ocular therapeutics. *Advanced Drug Delivery Reviews* **62**: 100-117.

DelMonte, D. W., Kim, T. 2011. Anatomy and physiology of the cornea. *Journal of Cataract & Refractive Surgery* **37**: 588-598.

Diebold, Y., Calonge, M. 2010. Applications of nanoparticles in ophthalmology. *Progress in Retinal and Eye Research* **29**: 596-609.

Ding, S. 1998. Recent developments in opththalmic drug delivery. *PSTT* **1** (8): 328-335.

Dvorchik, B. H., Brazier, D., DeBruin, M. F., Arbeit, R. D. 2002. Daptomycin Pharmacokinetics and Safety following Administration of Escalating Doses Once Daily to Healthy Subjects. *Antimicrobial Agents and Chemotherapy* **47**: 1318 – 1323.

Eljarrat-Binstock, E., Orucov, F., Aldouby, Y., Frucht-Pery, J., Domb, A. J. 2007. Charged nanoparticles delivery to the eye using hydrogel iontophoresis. *Journal of Controlled Release* **126**: 156-161.

Enoch, D. A., Bygott, J. M., Daly, M., Karas, J. A. 2007. Daptomycin. *Journal of Infection* **55**: 205-213.

European Centre for Disease Prevention and Control. 2013. Susceptibility of Enterococcus faecium isolates to vancomycin in participating countries in 2011. Available: http://www.ecdc.europa.eu [October 21, 2013].

Fuchs, P. C., Barry, A. L., Brown, S. D. 2002. In vitro bactericidal activity of daptomycin against staphylococci. *Journal of Antimicrobial Chemotherapy* **49** (3): 467 – 470.

Gaudana, R., Ananthula, H. K., Parenky, A., Mitra, A. K. 2010. Ocular Drug Delivery. *The American Association of Pharmaceutical Scientists Journal*. **12** (3): 348-360.

Geiger, R. C., Waters, C. M., Kamp, D. W., Glucksberg, M. R. 2005. KGF prevents oxygen-mediated damage in ARPE-19 cells. Investigative Ophthalmology & Visual Science 49 (9): 3435 – 3442.

Hamman, J. H. 2010. Chitosan based polyelectrolyte complexes as potential carrier materials in drug delivery systems. *Marine Drugs* **8**: 1305 - 1322.

Hans, M. L., Lowman, A. M. 2002. Biodegradable nanoparticles for drug delivery and targeting. *Current Opinion in Solid State and Materials Science* **6**: 319-327.

Harnsilawat, T., Pongsawatmanit, R., McClements, D. J. 2006. Characterization of β-lactoglobulin-sodium alginate interactions in aqueous solutions: a calorimetry, light-scattering, electrophoretic mobility and solubility study. *Food Hydrocolloids* **20** (5): 577-585.

Hornof, M., Toropainen, E., Urtti, A. 2005. Cell culture models of the ocular barriers. *European Journal of Pharmaceutics and Biopharmaceutics* **60**: 207 – 225.

Järvinen, K., Järvinen, T., Urtti, A. 1995. Ocular Absorption following topical delivery. *Advanced Drug Delivery Reviews* **16**: 3-19.

Jeu, L., Fung, H. B. 2004. Daptomycin: A Cyclic Lipopeptide Antimicrobial Agent. *Clinical Therapeuthics* **26** (11): 1728-1757.

Kernt, M., Kampik, A. 2010. Endophthalmitis: Pathogenesis, clinical presentation, management, and perspectives. *Clinical Ophthalmology* **4**: 121 – 135.

Klyce, S. D., Cronsson, C. E. 1985. Transport processes across the rabbit corneal epithelium: a review. *Current Eye Research* **4**: 323 – 331.

Kong, M., Chen, X. G., Xing, K., Park, H. J. 2010. Antimicrobial properties of chitosan and mode of action: a state of art review. *International Journal of Food Microbiology* **144**: 51-63.

Kunimoto, D. Y., Das, T., Sharma, S., Jalali, S., Majji, A., Gopinathan U., Athmanathan, S., Rao, T. N. 1999 Microbiologic Spectrum and Susceptibility of Isolates : Part I. Postoperative Endophthalmitis. *American Journal of Ophthalmology* **128** (2): 240 – 242.

Le Bourlais, C., Acar, L., Zia, H., Sado, P., Needham, T., Leverge, R. 1998. Ophthalmic Drug Delivery Systems – Recent Advances, *Progress in Retinal and Eye Research* **17**(1): 33-58.

Liew, C. V., Chan, L. W., Ching, A. L., Heng, P. W. S. 2005. Evaluation of sodium alginate as drug release modifier in matrix tablets. *International Journal of Pharmaceutics* **309**: 25-37.

Liu, S., Jones, L., Gu, F. X. 2012 Nanomaterials for ocular drug delivery. *Macromolecular Bioscience* **12**: 608-620.

Liu, W., Griffith, M., Li, F. 2008. Alginate microsphere-collagen composite hydrogel for ocular drug delivery and implantation. *Journal of Materials Science and Materials in Medicine* **19** (11): 3365-3371.

Liu, Z., Li, J., Nie, S., Liu, H., Ding, P., Pan, W. 2006. Study of alginate/HPMC-based in situ gelling ophthalmic delivery system for gatifloxacin. *International Journal of Pharmaceutics* **315** (1 -2): 12-17.

Ludwig, A. 2005. The use of mucoadhesive polymers in ocular drug delivery. *Advanced Drug Delivery Reviews* **57**: 1597-1639.

Malhotra, A., Minja, F. J., Crum, A., Burrowes, D. 2011. Ocular Anatomy and Cross-Sectional Imaging of the Eye. *Seminars in Ultrasound CT and MRI* **32**:2-13.

Martens-Lobenhoffer, J., Kielstein, J. T., Oye, C., Bode-Böger, S. M. 2008. Validated high performance liquid chromatography-UV detection method for determination of daptomycin in human plasma. *Journal of Chromatography B* **875**: 546-550

McKinnell, J., Kunz, D., Chamot, E., Patel, M., Shirley, R., Moser, S., Baddley, J., Pappas, P., Miller, L. 2012. Association between Vancomycin-resistant Enterococci Bacteremia and Ceftriaxone Usage. *Infection Control and Hospital Epidemiology* **33** (7): 718 – 724.

Motwani, S. K., Chopra, S., Talegaonkar, S., Kohli, K., Ahmad, F. J., Khar, R. K. 2007. Chitosan-sodium alginate nanoparticles as submicroscopic reservoirs for ocular delivery: formulation, optimization and *in vitro* characterization. *European Journal of Pharmaceutics and Biopharmaceutics* **68**: 513-525.

Nagarwal, R. C., Kumar, R., Pandit, J. K. 2012. Chitosan coated sodium alginate-chitosan nanoparticles loaded with 5-FU for ocular delivery: *in vitro* characterization and *in vivo* study in rabbit eye. *European Journal of Pharmaceutical Sciences* **47**:678-685.

Nagpal, K., Singh, S. K., Mishra, D. N. 2010. Chitosan nanoparticles: a promising system in novel drug delivery. *Chemical and Pharmaceutical Bulletin* **58** (11): 1423-1430.

Nguyen, K. T., Ritz, D., Gu, J., Alexander, D., Chu, M., Miao, V., Brian, P., Baltz, R. H. 2006. Combinatorial biosynthesis of novel antibiotics related to daptomycin. *Proceedings of the National Academy of Sciences* **103** (46): 17462-17467.

Park, J., Zhang, Y., Vykhodtseva, N., Akula, J. D., McDannold, N. J. 2012. Targeted and reversible blood-retinal barrier disruption via focused ultrasound and microbubbles. *Public Library of Science* **7** (8): 1-8.

Patil, J. S., Kamalapur, M. V., Marapur, S. C., Kadam, D. V. 2010. Ionotropic gelation and polyelectrolyte complexation: the novel techniques to design hydrogel particulate sustained, modulated drug delivery system: a review. *Digest Journal of Nanomaterials and Biostructures* **5** (1): 241 - 248.

Peyman, G. A., Lee, P. J., Seal, D. V. 2004. Endophthalmitis: Diagnosis and Treatment, 1st edition. Taylor & Francis, Oxfordshire, pp. 101.

Presland, A. 2007. Applied Ocular Physiology and Anatomy. *Anaesthesia and Intensive Care Medicine* **8** (9): 379-381.

Robinson, J. R., Mlynek, G. M. 1995. Bioadhesive and phase-change polymers for ocular drug delivery. *Advanced Drug Delivery Reviews* **16**: 45-50.

Sangeetha, S., Venkatesh, D. N., Adhiyaman, R., Santhi, K., Suresh, B. 2007. Formulation of sodium alginate nanospheres containing Amphotericin B for the treatment of systemic candidiasis. *Tropical Journal of Pharmaceutical Research* **6** (1): 653-659.

Sarmento, B., Ribeiro, A., Veiga, F., Sampaio, P., Neufeld, R and Ferreira, D. 2007. Alginate/ chitosan nanoparticles are effective for oral insulin delivery. *Pharmaceutical Research* **24** (12): 2198 – 2206.

Sheedlo, H., Li, L., Turner, J. 1992. Effects of RPE-cell factors secreted from permselective fibers on retinal cells in vitro. *Brain Research* **587**: 327 – 337.

Short, B. 2008. Safety Evaluation of Ocular Drug Delivery Formulations: Techniques and Pratical Considerations. *Toxicologic Pathology* **36**: 49-62.

Silva, N., Silva, S., Sarmento, B., Pintado, M. 2013. Chitosan nanoparticles for daptomycin delivery in ocular treatment of bacterial endophthalmitis. *Drug Delivery* ID: 858195 DOI:10.3109/10717544.2013.858195 – accepted.

Tanjak, P., Ngamviriyavong, P., Janvikul, W. 2011. Antibacterial and Cytotoxicity of Chitosan and Quaternized Chitosans. Pure and Applied Chemistry International Conference. Thailand.

The College of Optometrists. 2011. Endophthalmitis (post-operative): Exogenous endopthalmitis. London, United Kingdom

Thrimawithana, T. K., Young, S., Bunt, C. R., Green, C., Alany, R. G. 2011. Drug delivery to the posterior segment of the eye. *Drug Discovery Today* **16** (5/6): 270-277.

Tønnesen, H., Karlsen, J. 2002. Alginate in Drug Delivery Systems. *Drug Development and Industrial Pharmacy* **28** (6): 621 -630.

Urtti, A. 2006. Challenges and obstacles of ocular pharmacokinetics and drug delivery. *Advanced Drug Delivery Reviews* **58**: 1131-1135.

Zahoor, A., Sharma, S., Khuller, G. K. 2005. Inhalable alginate nanoparticles as antitubercular drug carriers against experimental tuberculosis. *International Journal of Antimicrobial Agents* **26** (4): 298-303.

Zahoor, A., Sharma, S., Khuller, G. K. 2007. Chemotherapeutic evaluation of alginate nanoparticle-encapsulated azole antifungal and antitubercular drugs against murine tuberculosis. *Nanomedicine: Nanotechnology, Biology, and Medicine* **3**: 239 - 243

Zarbin, M. A., Montemagno, C., Leary, J. F., Ritch, R. 2010. Nanomedicine in ophthalmology: the new frontier. *American Journal of Ophthalmology* **150**: 144 - 162.

Zhu, X., Su, M., Tang, S., Wang, L., Liang, X., Meng, F., Hong, Y., Xu, Z. 2012. Synthesis of thiolated chitosan and preparation nanoparticles with sodium alginate for ocular drug delivery. *Molecular Vision* **18**: 1973-1982.

Zimmer, A., Kreuter, J. 1995. Microspheres and nanoparticles used in ocular delivery systems. *Advanced Drug Delivery Reviews* **16**: 61 - 73.

Watkins, R. R., Lemonovich, T. L., File Jr., T. M. 2012. An evidence-based review of linezolid for the treatment of methicillin-resistant *Staphylococcus aureus* (MRSA): place in therapy. *Core Evidence* **7**: 131-143